

Tracking saddle-to-scission dynamics using N/Z in projectile breakup reactions

SYLVIE HUDAN

September 4, 2012



Nuclear Equation of State

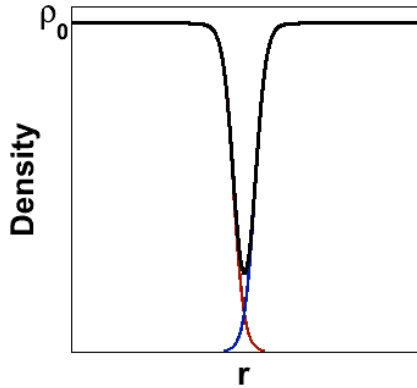
$$E(\rho, \delta) = E(\rho, \delta = 0) + E_{sym}(\rho)\delta^2 \quad \delta = \frac{\rho_n - \rho_p}{\rho_{Total}}$$

→ Migration of neutron to low-density region

Nuclear Equation of State

$$E(\rho, \delta) = E(\rho, \delta = 0) + E_{sym}(\rho)\delta^2 \quad \delta = \frac{\rho_n - \rho_p}{\rho_{Total}}$$

→ Migration of neutron to low-density region

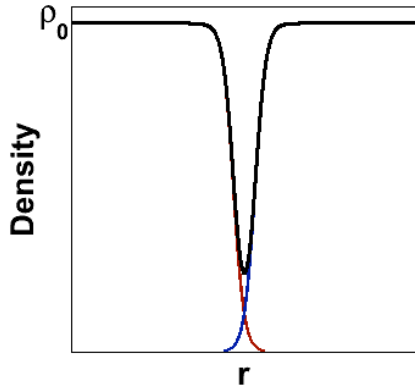


→ Low-density density always present between two interacting nuclei

Nuclear Equation of State

$$E(\rho, \delta) = E(\rho, \delta = 0) + E_{sym}(\rho)\delta^2 \quad \delta = \frac{\rho_n - \rho_p}{\rho_{Total}}$$

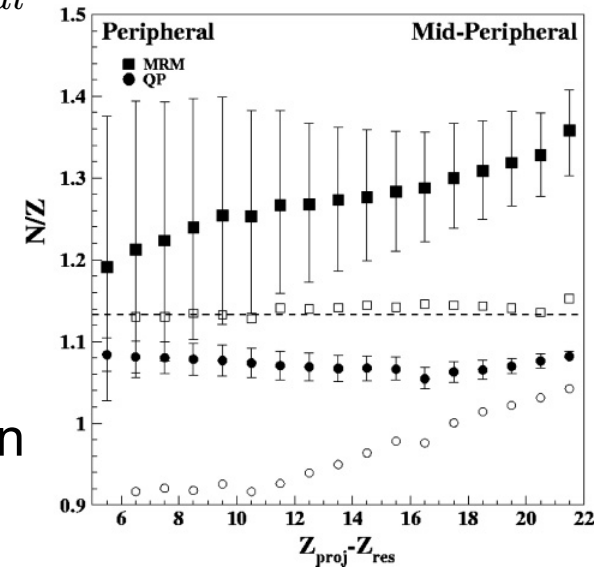
→ Migration of neutron to low-density region



→ Low-density density always present between two interacting nuclei

→ Observation of n-rich material in overlap region for a **symmetric** system

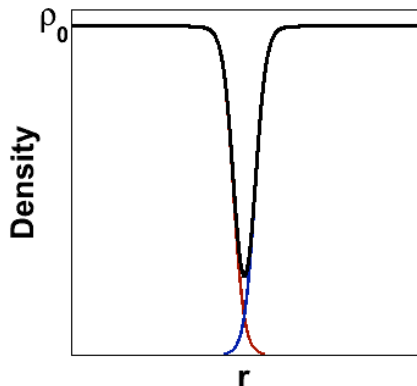
$^{64}\text{Zn} + ^{64}\text{Zn}$ @ 45 MeV/A



Nuclear Equation of State

$$E(\rho, \delta) = E(\rho, \delta = 0) + E_{sym}(\rho)\delta^2 \quad \delta = \frac{\rho_n - \rho_p}{\rho_{Total}}$$

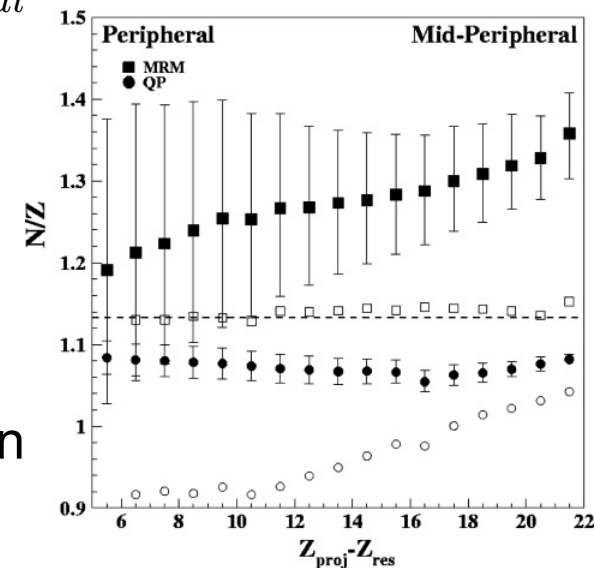
→ Migration of neutron to low-density region



→ Low-density density always present between two interacting nuclei

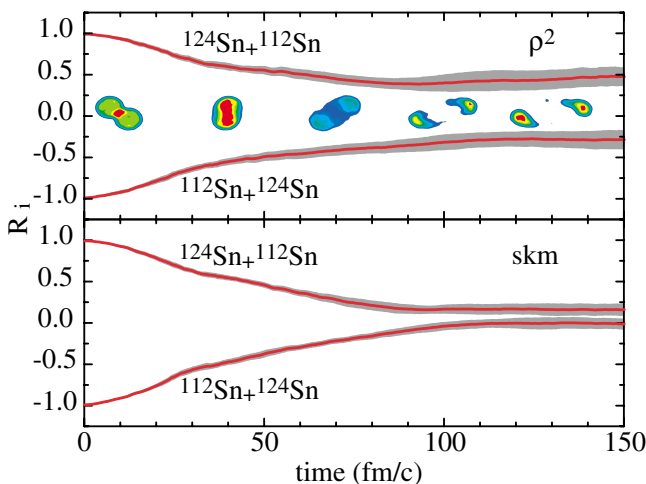
→ Observation of n-rich material in overlap region for a **symmetric** system

$^{64}\text{Zn} + ^{64}\text{Zn}$ @ 45 MeV/A



Collisions of N/Z asymmetric nuclei

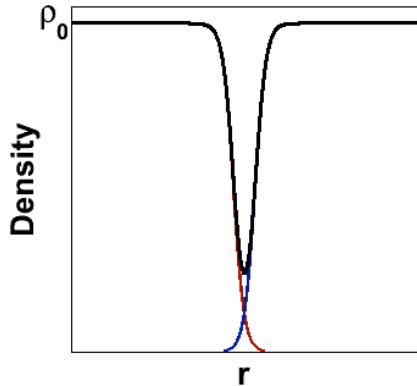
→ Short times



Nuclear Equation of State

$$E(\rho, \delta) = E(\rho, \delta = 0) + E_{sym}(\rho)\delta^2 \quad \delta = \frac{\rho_n - \rho_p}{\rho_{Total}}$$

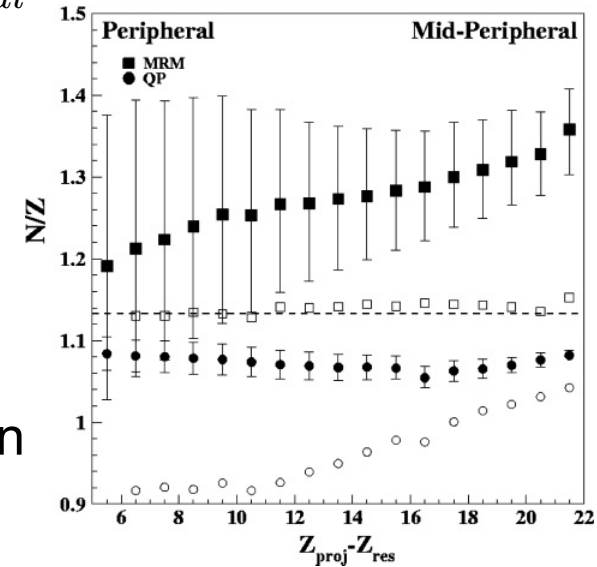
→ Migration of neutron to low-density region



→ Low-density density always present between two interacting nuclei

→ Observation of n-rich material in overlap region for a **symmetric** system

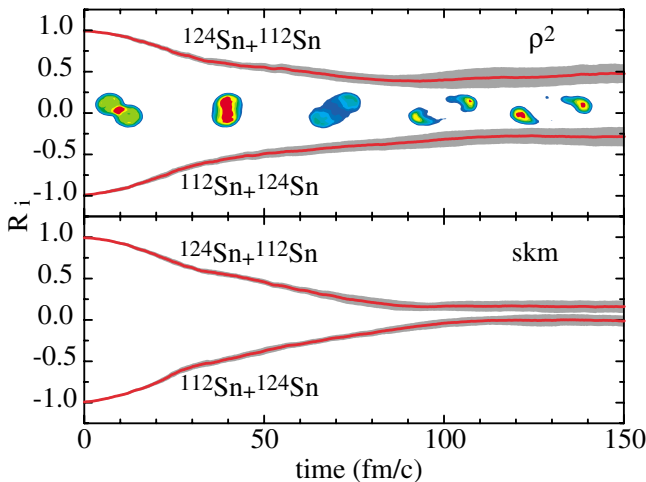
$^{64}\text{Zn} + ^{64}\text{Zn}$ @ 45 MeV/A



Collisions of N/Z asymmetric nuclei

→ Short times

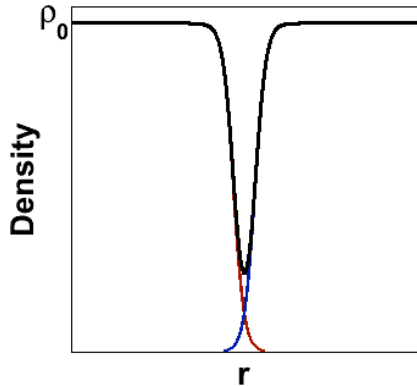
Ideally: Long-lived system



Nuclear Equation of State

$$E(\rho, \delta) = E(\rho, \delta = 0) + E_{sym}(\rho)\delta^2 \quad \delta = \frac{\rho_n - \rho_p}{\rho_{Total}}$$

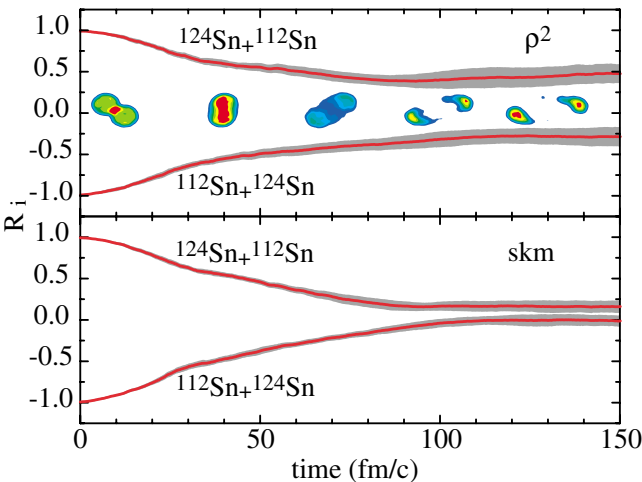
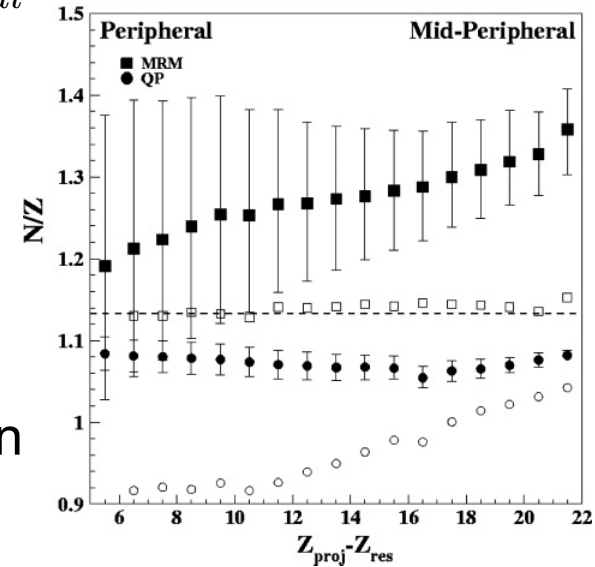
→ Migration of neutron to low-density region



→ Low-density density always present between two interacting nuclei

→ Observation of n-rich material in overlap region for a **symmetric** system

$^{64}\text{Zn} + ^{64}\text{Zn}$ @ 45 MeV/A



Collisions of N/Z asymmetric nuclei

→ Short times

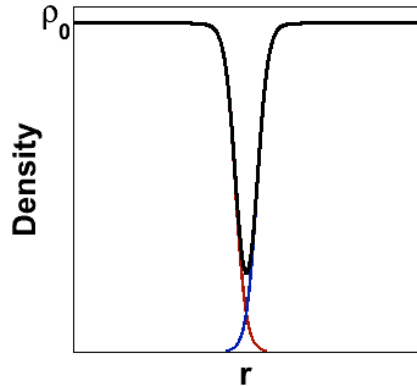
Ideally: Long-lived system

→ Damped collisions

Nuclear Equation of State

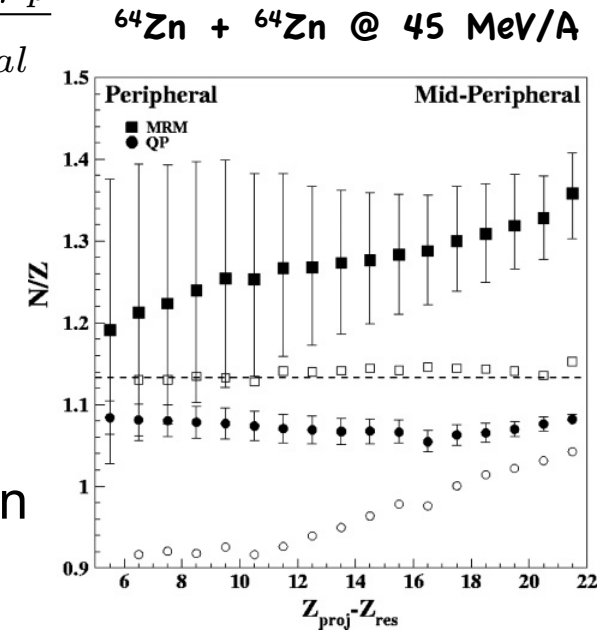
$$E(\rho, \delta) = E(\rho, \delta = 0) + E_{sym}(\rho)\delta^2 \quad \delta = \frac{\rho_n - \rho_p}{\rho_{Total}}$$

→ Migration of neutron to low-density region



→ Low-density density always present between two interacting nuclei

→ Observation of n-rich material in overlap region for a **symmetric** system



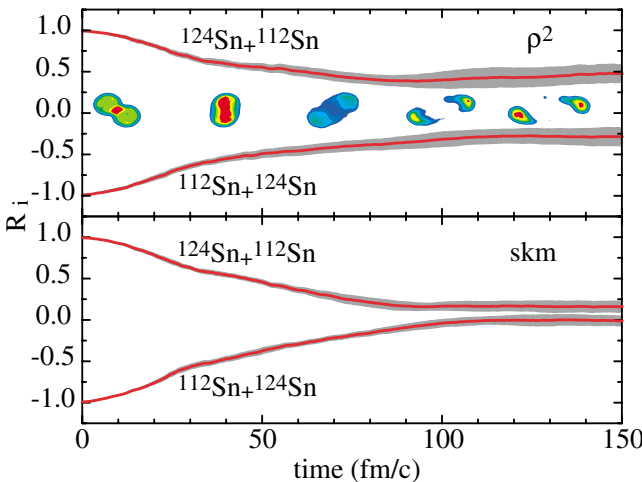
Collisions of N/Z asymmetric nuclei

→ Short times

Ideally: Long-lived system

→ Damped collisions

→ **Binary decay of PLF***



PLF* Binary Decay

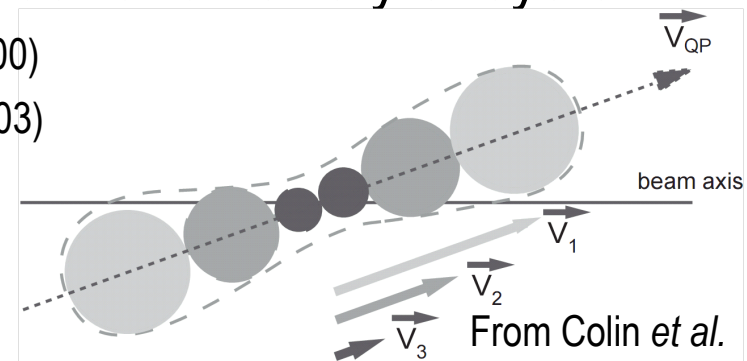
PLF* Binary Decay

- Process with a large cross-section, observed for a variety of systems

Montoya *et al.*, PRL**73**, 3070 (1994); Bocage *et al.*, NPA**676**, 391 (2000)

Davin *et al.*, PRC**65**, 064614 (2002); Colin *et al.*, PRC**67**, 064603 (2003)

McIntosh *et al.*, PRC**81**, 034603 (2010)



PLF* Binary Decay

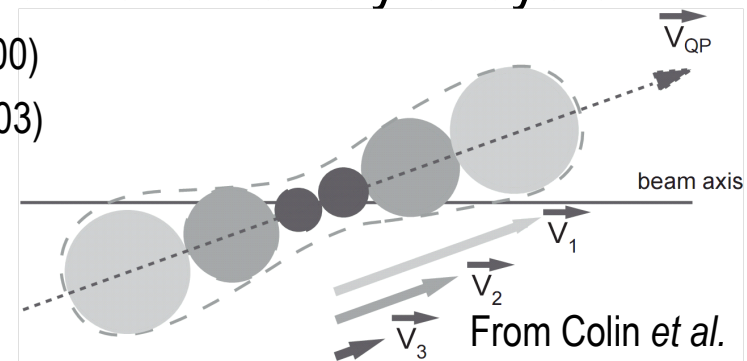
- Process with a large cross-section, observed for a variety of systems

Montoya *et al.*, PRL**73**, 3070 (1994); Bocage *et al.*, NPA**676**, 391 (2000)

Davin *et al.*, PRC**65**, 064614 (2002); Colin *et al.*, PRC**67**, 064603 (2003)

McIntosh *et al.*, PRC**81**, 034603 (2010)

- Selectable size, initial N/Z



PLF* Binary Decay

- Process with a large cross-section, observed for a variety of systems

Montoya *et al.*, PRL73, 3070 (1994); Bocage *et al.*, NPA676, 391 (2000)

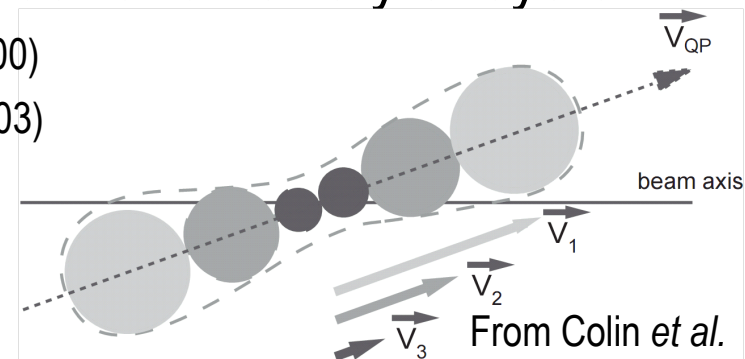
Davin *et al.*, PRC65, 064614 (2002); Colin *et al.*, PRC67, 064603 (2003)

McIntosh *et al.*, PRC81, 034603 (2010)

- Selectable size, initial N/Z

- Angular momentum

- Rotation angle can be used as a “clock”



PLF* Binary Decay

- Process with a large cross-section, observed for a variety of systems

Montoya *et al.*, PRL73, 3070 (1994); Bocage *et al.*, NPA676, 391 (2000)

Davin *et al.*, PRC65, 064614 (2002); Colin *et al.*, PRC67, 064603 (2003)

McIntosh *et al.*, PRC81, 034603 (2010)

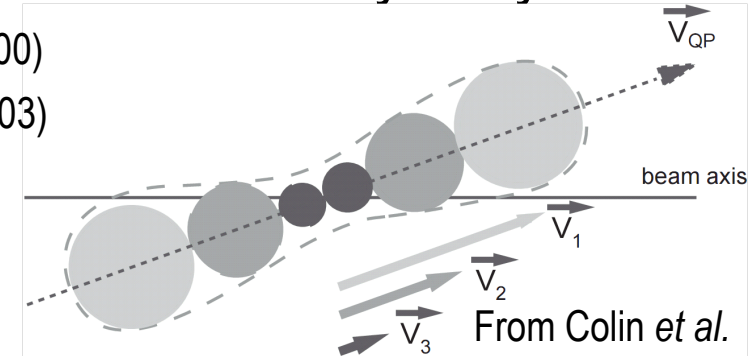
- Selectable size, initial N/Z

- Angular momentum

- Rotation angle can be used as a “clock”

- Relatively long-lived system (> 100 fm/c)

Casini *et al.*, PRL71, 2567 (1993); Piantelli *et al.*, RPL88, 052701 (2002)



PLF* Binary Decay

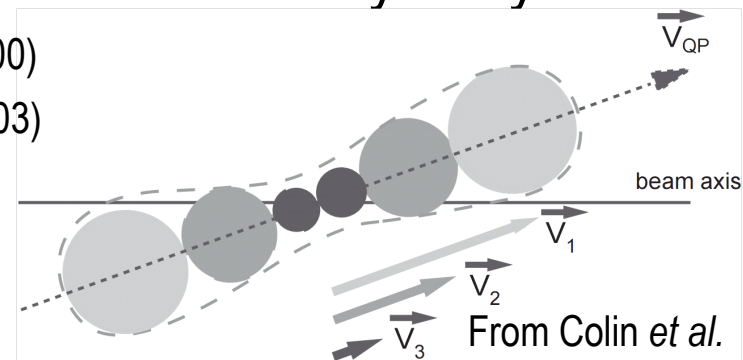
- Process with a large cross-section, observed for a variety of systems

Montoya *et al.*, PRL73, 3070 (1994); Bocage *et al.*, NPA676, 391 (2000)

Davin *et al.*, PRC65, 064614 (2002); Colin *et al.*, PRC67, 064603 (2003)

McIntosh *et al.*, PRC81, 034603 (2010)

- Selectable size, initial N/Z
- Angular momentum
 - Rotation angle can be used as a “clock”
- Relatively long-lived system (> 100 fm/c)
 - Casini *et al.*, PRL71, 2567 (1993); Piantelli *et al.*, RPL88, 052701 (2002)
- Fragments emitted near the projectile velocity



PLF* Binary Decay

- Process with a large cross-section, observed for a variety of systems

Montoya *et al.*, PRL73, 3070 (1994); Bocage *et al.*, NPA676, 391 (2000)

Davin *et al.*, PRC65, 064614 (2002); Colin *et al.*, PRC67, 064603 (2003)

McIntosh *et al.*, PRC81, 034603 (2010)

- Selectable size, initial N/Z

- Angular momentum

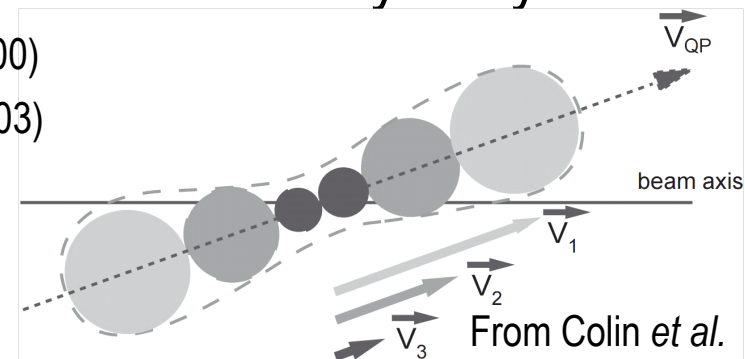
- Rotation angle can be used as a “clock”

- Relatively long-lived system (> 100 fm/c)

Casini *et al.*, PRL71, 2567 (1993); Piantelli *et al.*, RPL88, 052701 (2002)

- Fragments emitted near the projectile velocity

- **Not** mid-rapidity emission



PLF* Binary Decay

- Process with a large cross-section, observed for a variety of systems

Montoya *et al.*, PRL73, 3070 (1994); Bocage *et al.*, NPA676, 391 (2000)

Davin *et al.*, PRC65, 064614 (2002); Colin *et al.*, PRC67, 064603 (2003)

McIntosh *et al.*, PRC81, 034603 (2010)

- Selectable size, initial N/Z

- Angular momentum

- Rotation angle can be used as a “clock”

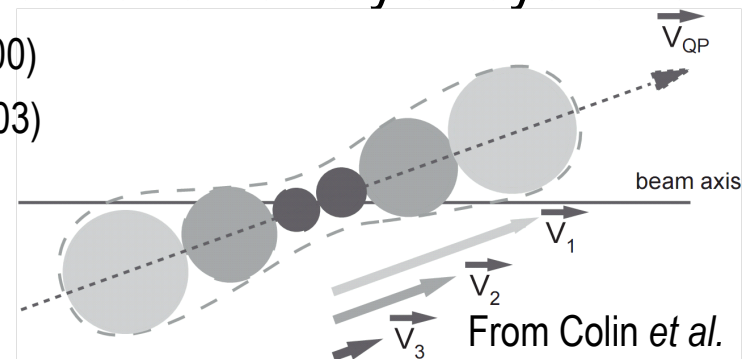
- Relatively long-lived system (> 100 fm/c)

Casini *et al.*, PRL71, 2567 (1993); Piantelli *et al.*, RPL88, 052701 (2002)

- Fragments emitted near the projectile velocity

- **Not** mid-rapidity emission

- The system is not in close proximity with the target but could be influenced by the target Coulomb field



Experimental Setup

$^{124(,136)}\text{Xe} + ^{112, 124}\text{Sn} @ 49.2 \text{ MeV/A}$

Experiment performed at GANIL (France)

N/Z

^{124}Xe	^{124}Sn	^{112}Sn
1.30	1.48	1.24

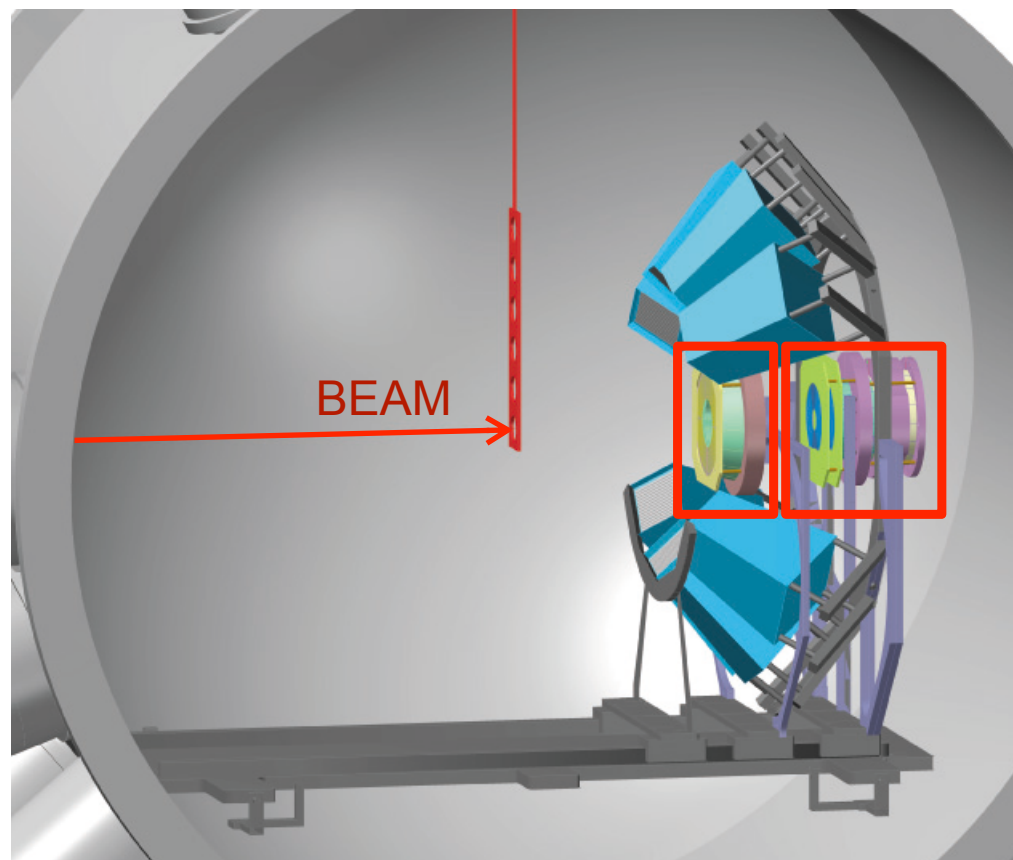
Experimental Setup

$^{124(,136)}\text{Xe} + ^{112, 124}\text{Sn} @ 49.2 \text{ MeV/A}$

Experiment performed at GANIL (France)

N/Z

^{124}Xe	^{124}Sn	^{112}Sn
1.30	1.48	1.24



Experimental Setup

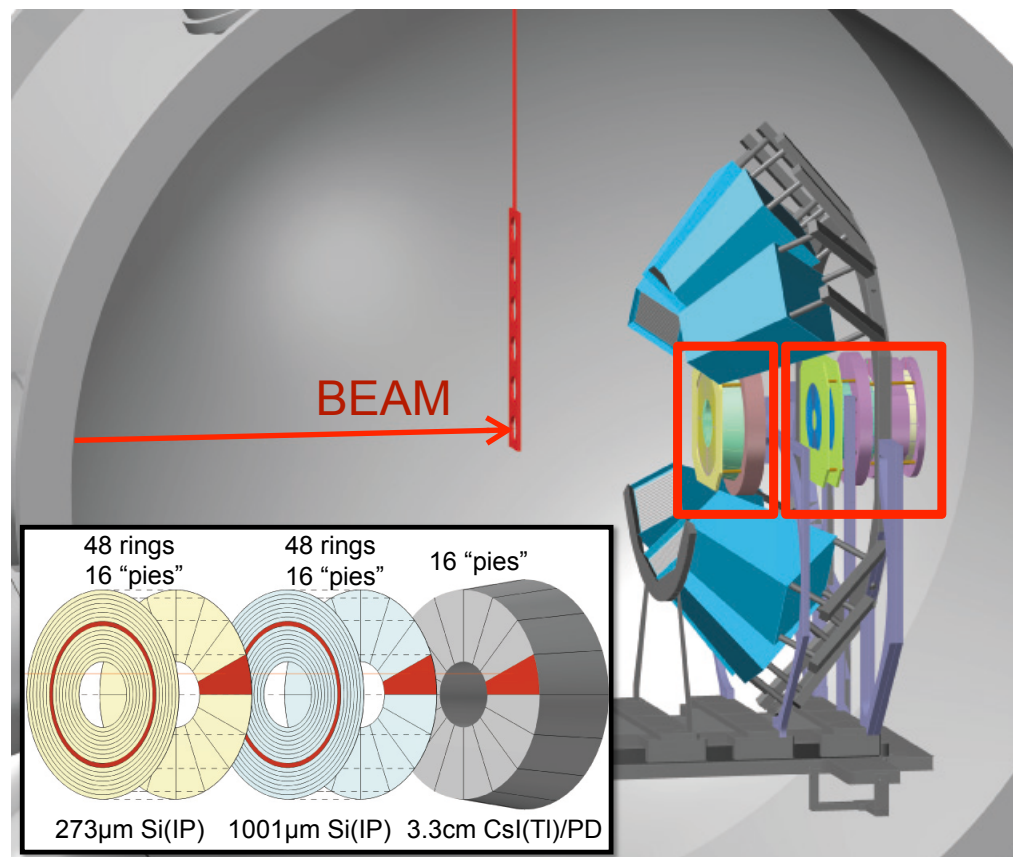
$^{124(,136)}\text{Xe} + ^{112, 124}\text{Sn} @ 49.2 \text{ MeV/A}$

Experiment performed at GANIL (France)

N/Z

^{124}Xe	^{124}Sn	^{112}Sn
1.30	1.48	1.24

- T1: Si-Si-CsI(Tl)
 - $2.8^\circ \leq \theta_{\text{Lab}} \leq 6.6^\circ$
 - $Z = 1-55$; A for $Z = 1-14$



Experimental Setup

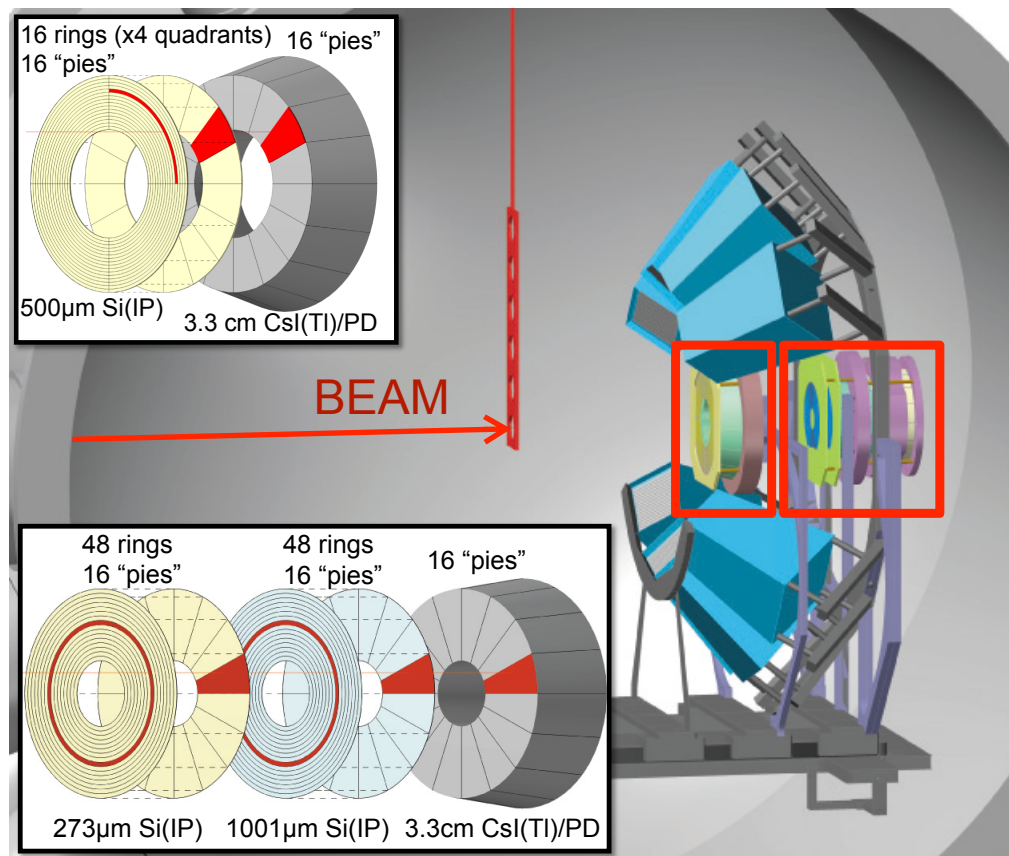
$^{124(,136)}\text{Xe} + ^{112, 124}\text{Sn} @ 49.2 \text{ MeV/A}$

Experiment performed at GANIL (France)

N/Z

^{124}Xe	^{124}Sn	^{112}Sn
1.30	1.48	1.24

- T1: Si-Si-CsI(Tl)
 - $2.8^\circ \leq \theta_{\text{Lab}} \leq 6.6^\circ$
 - $Z = 1-55$; A for $Z = 1-14$
- T2: Si-CsI(Tl)
 - $7.3^\circ \leq \theta_{\text{Lab}} \leq 14.3^\circ$
 - $Z = 1-24$; A for $Z=1-8$



Experimental Setup

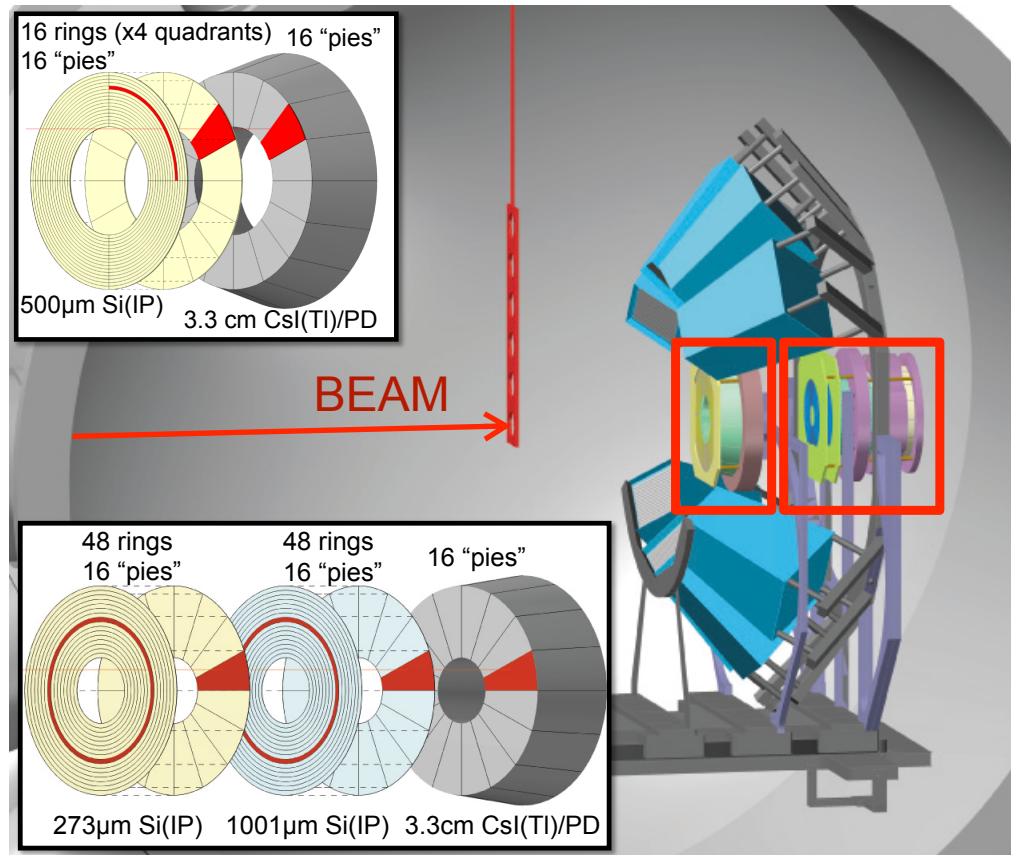
$^{124(,136)}\text{Xe} + ^{112, 124}\text{Sn} @ 49.2 \text{ MeV/A}$

Experiment performed at GANIL (France)

N/Z

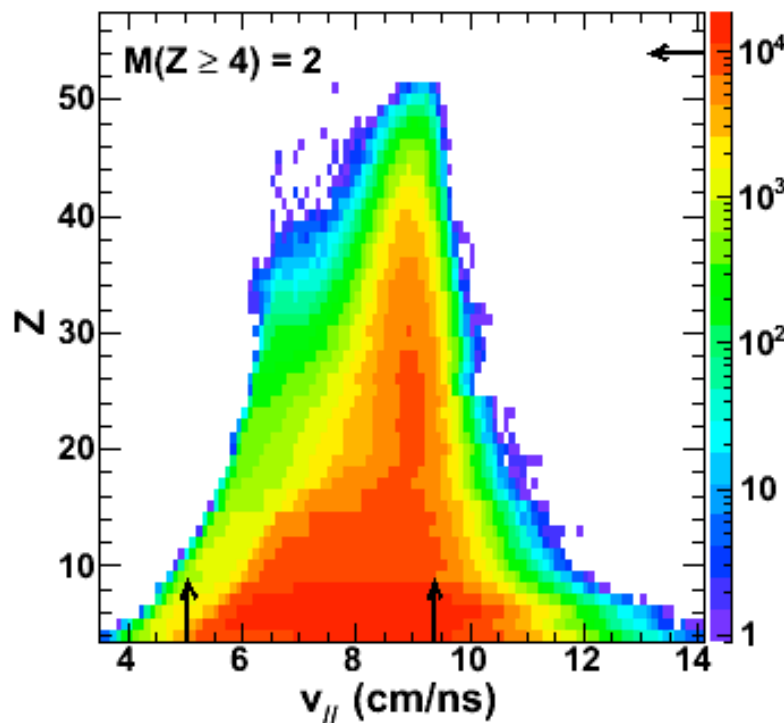
^{124}Xe	^{124}Sn	^{112}Sn
1.30	1.48	1.24

- T1: Si-Si-CsI(TI)
 - $2.8^\circ \leq \theta_{\text{Lab}} \leq 6.6^\circ$
 - $Z = 1-55$; A for $Z = 1-14$
- T2: Si-CsI(TI)
 - $7.3^\circ \leq \theta_{\text{Lab}} \leq 14.3^\circ$
 - $Z = 1-24$; A for $Z=1-8$
- LASSA: $36.4^\circ \leq \theta_{\text{Lab}} \leq 51.5^\circ$
- DEMON: n TOF



$^{124}\text{Xe} + ^{112}\text{Sn}$

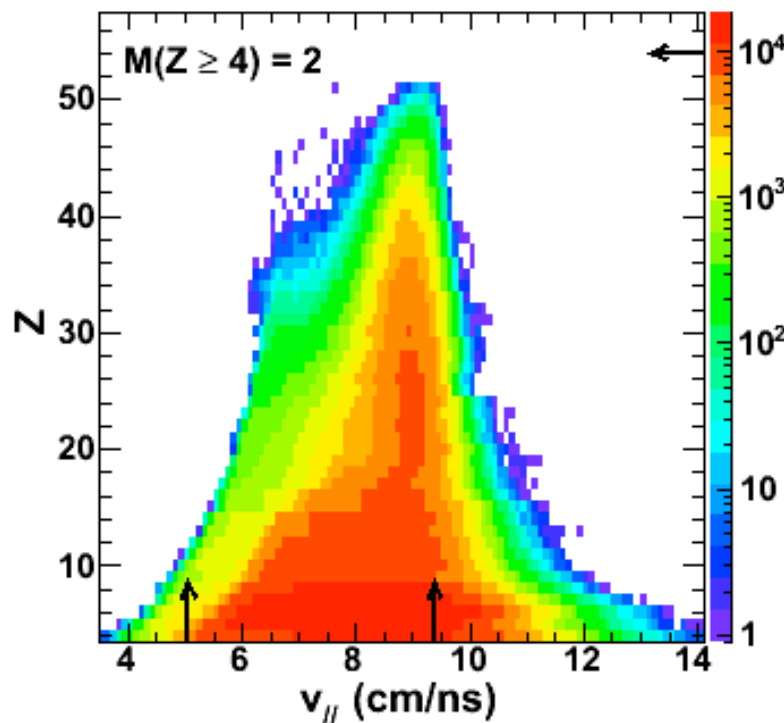
Event Characteristics

fragment: $Z \geq 4$ 

- Two fragment events characterized by large remanent PLF

$^{124}\text{Xe} + ^{112}\text{Sn}$

Event Characteristics

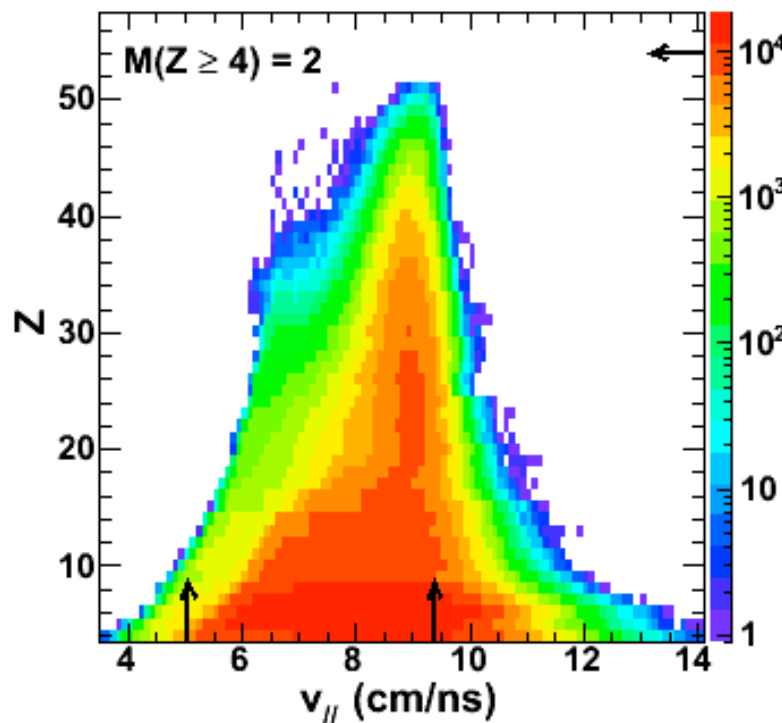
fragment: $Z \geq 4$ 

- Two fragment events characterized by large remanent PLF

Selection: $Z_{\text{Heavy}} > 20$

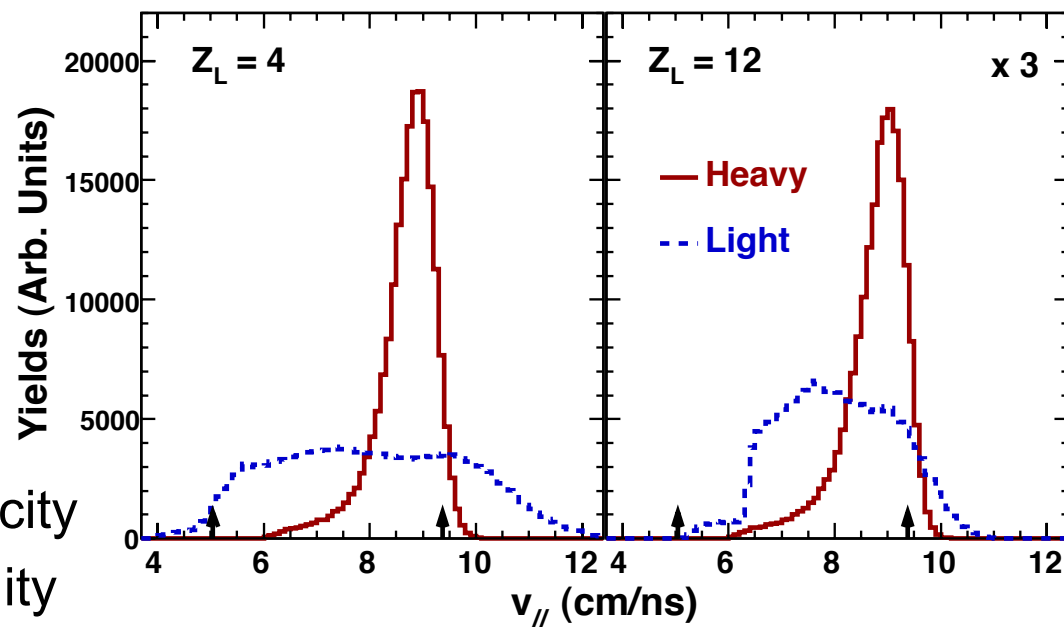
$^{124}\text{Xe} + ^{112}\text{Sn}$

Event Characteristics

fragment: $Z \geq 4$ 

- Two fragment events characterized by large remanent PLF

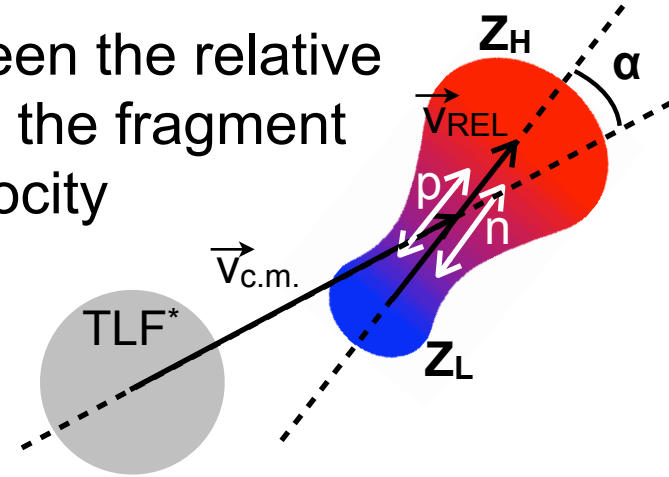
Selection: $Z_{\text{Heavy}} > 20$



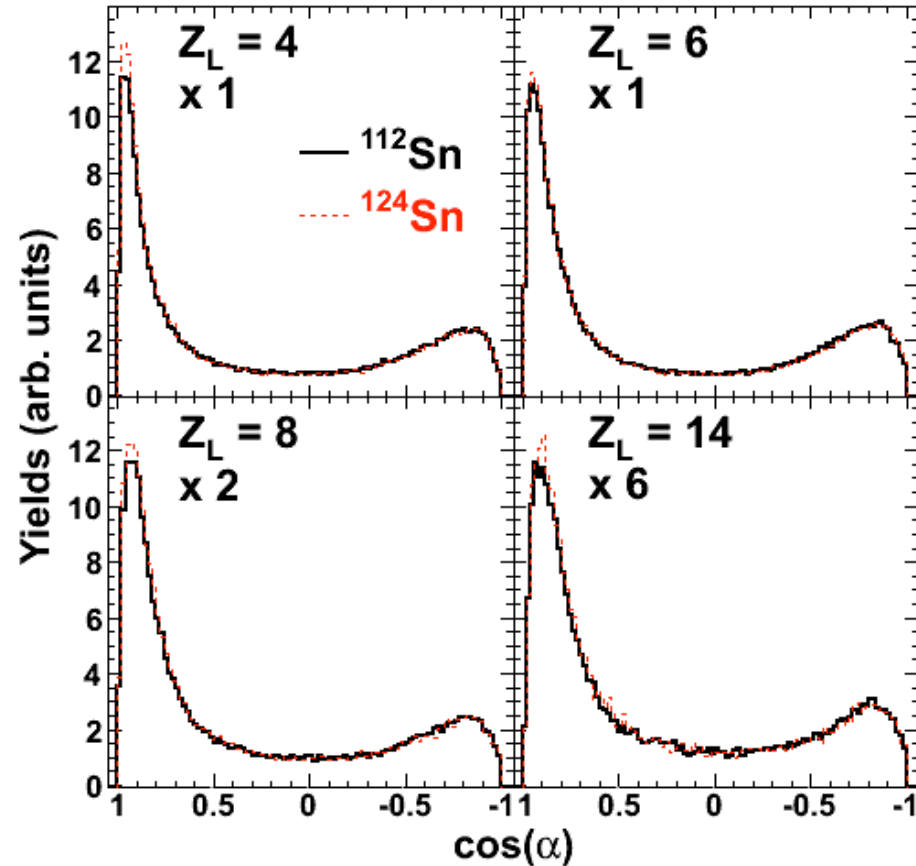
- Heavy fragment near beam velocity
- Light fragment **NOT** at mid-rapidity

Aligned Decay

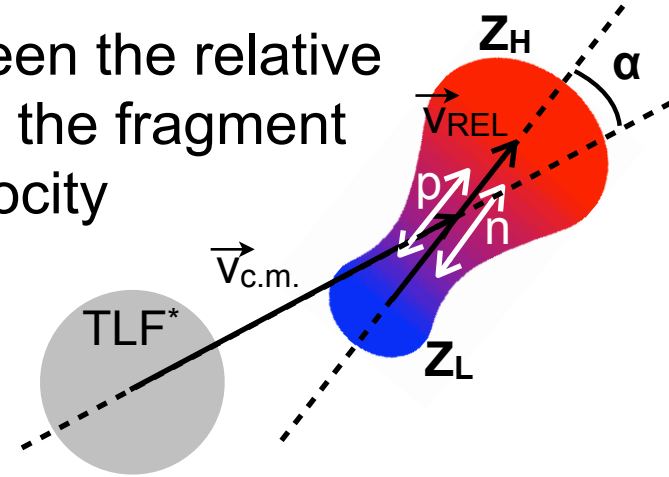
Angle between the relative velocity and the fragment "parent" velocity



Aligned Decay

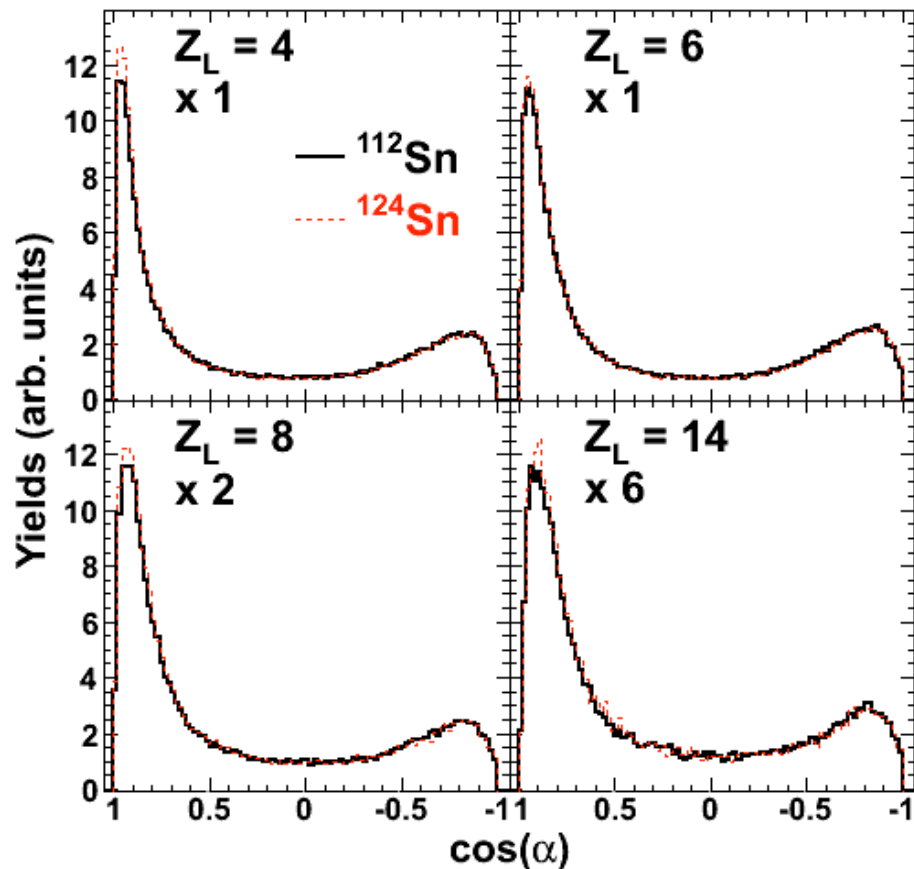

 $^{124}\text{Xe} + \text{Sn}$


Angle between the relative velocity and the fragment “parent” velocity

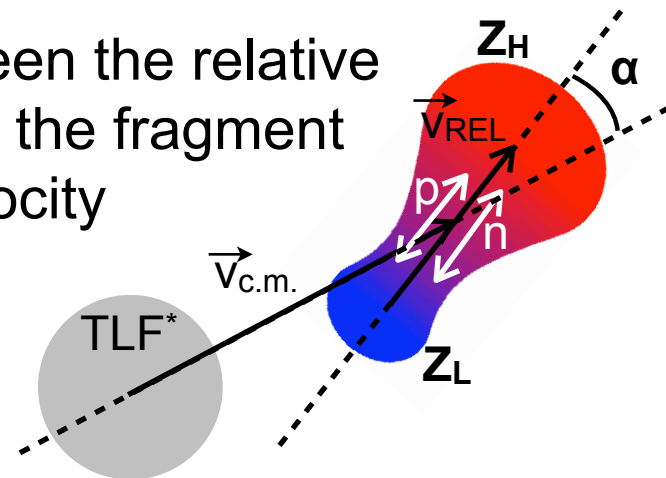


- Asymmetric angular distributions
- Larger asymmetry for lighter Z_L
- Asymmetry persists up to $Z_L = 18$
- Distributions similar for n-rich target

Aligned Decay


 $^{124}\text{Xe} + \text{Sn}$


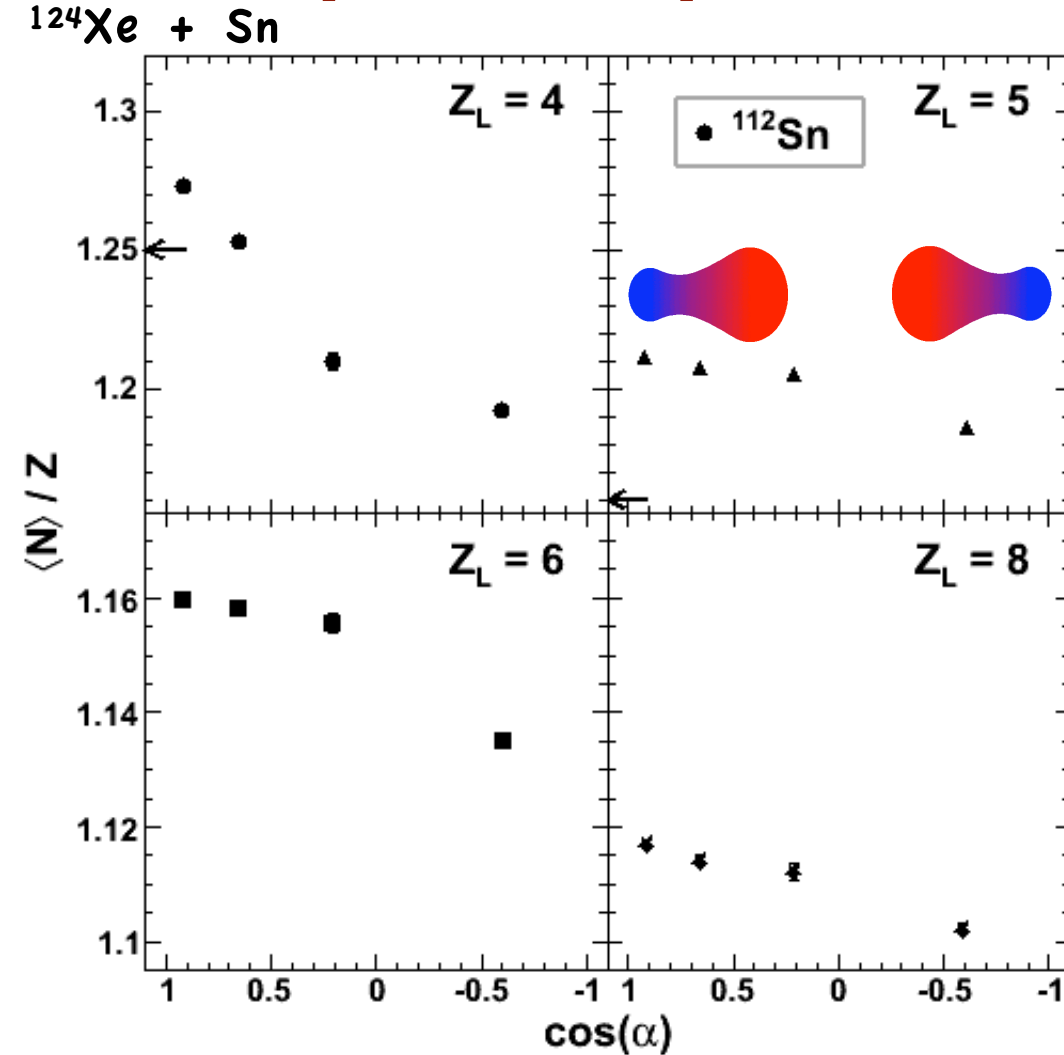
Angle between the relative velocity and the fragment “parent” velocity



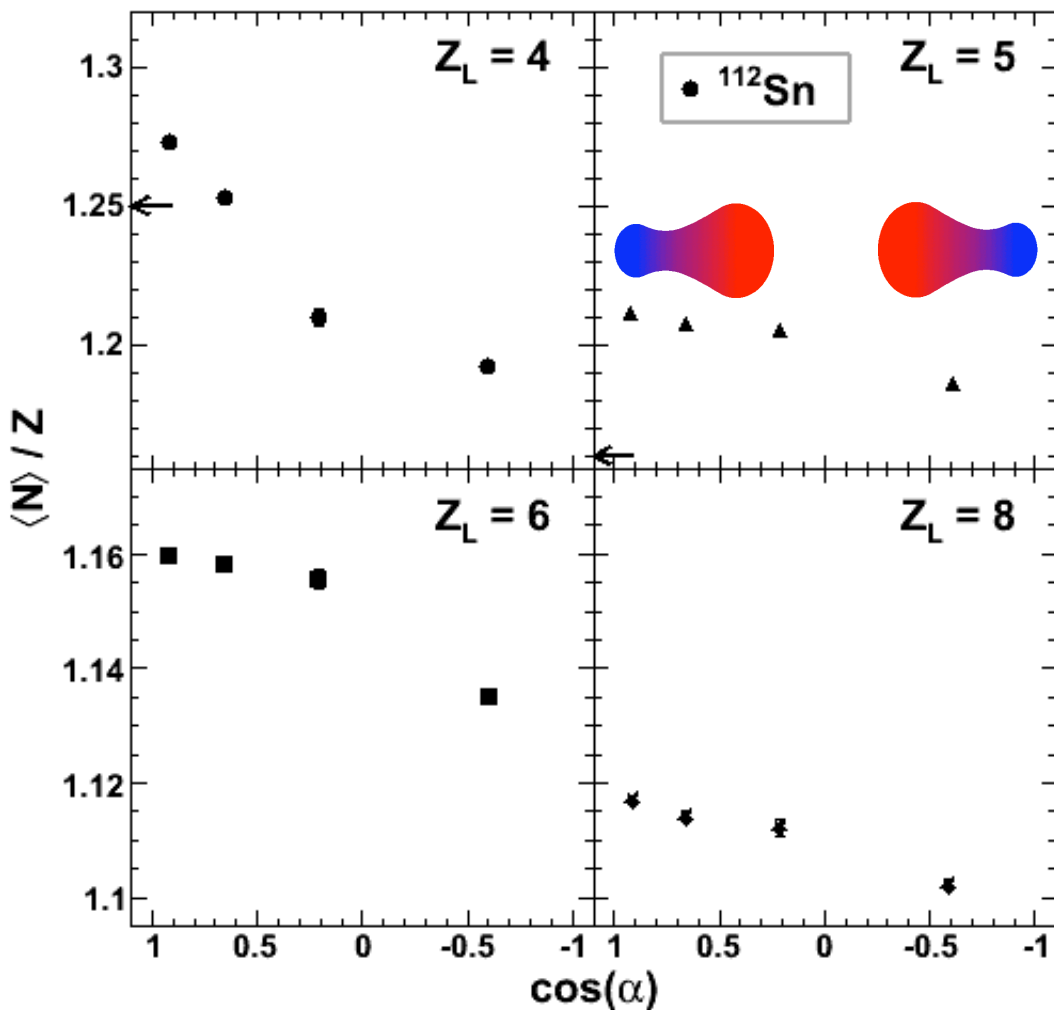
- Asymmetric angular distributions
- Larger asymmetry for lighter Z_L
- Asymmetry persists up to $Z_L = 18$
- Distributions similar for n-rich target

✎ *Backward enhancement observed in Sn+Ni for change of target and projectile**

Isotopic Composition vs Rotation Angle

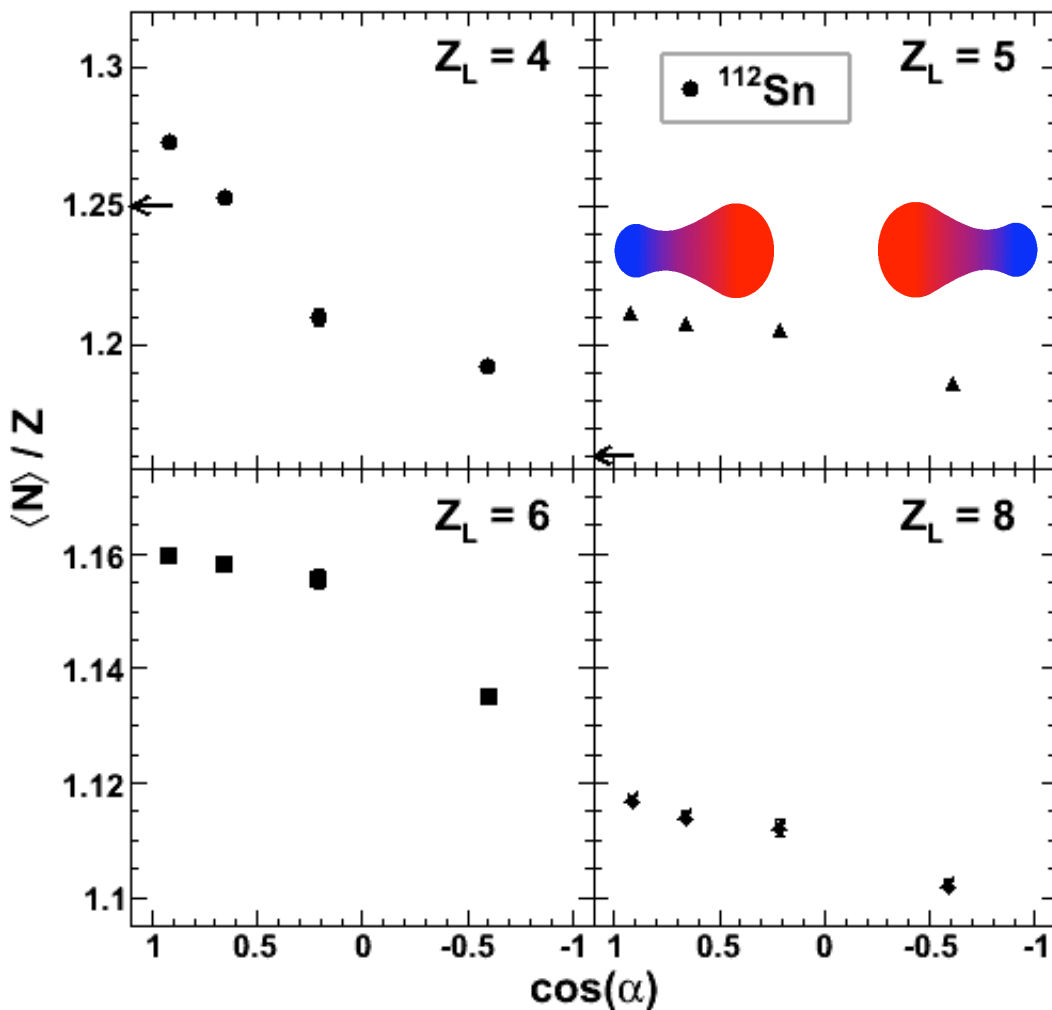


Isotopic Composition vs Rotation Angle

 $^{124}\text{Xe} + \text{Sn}$


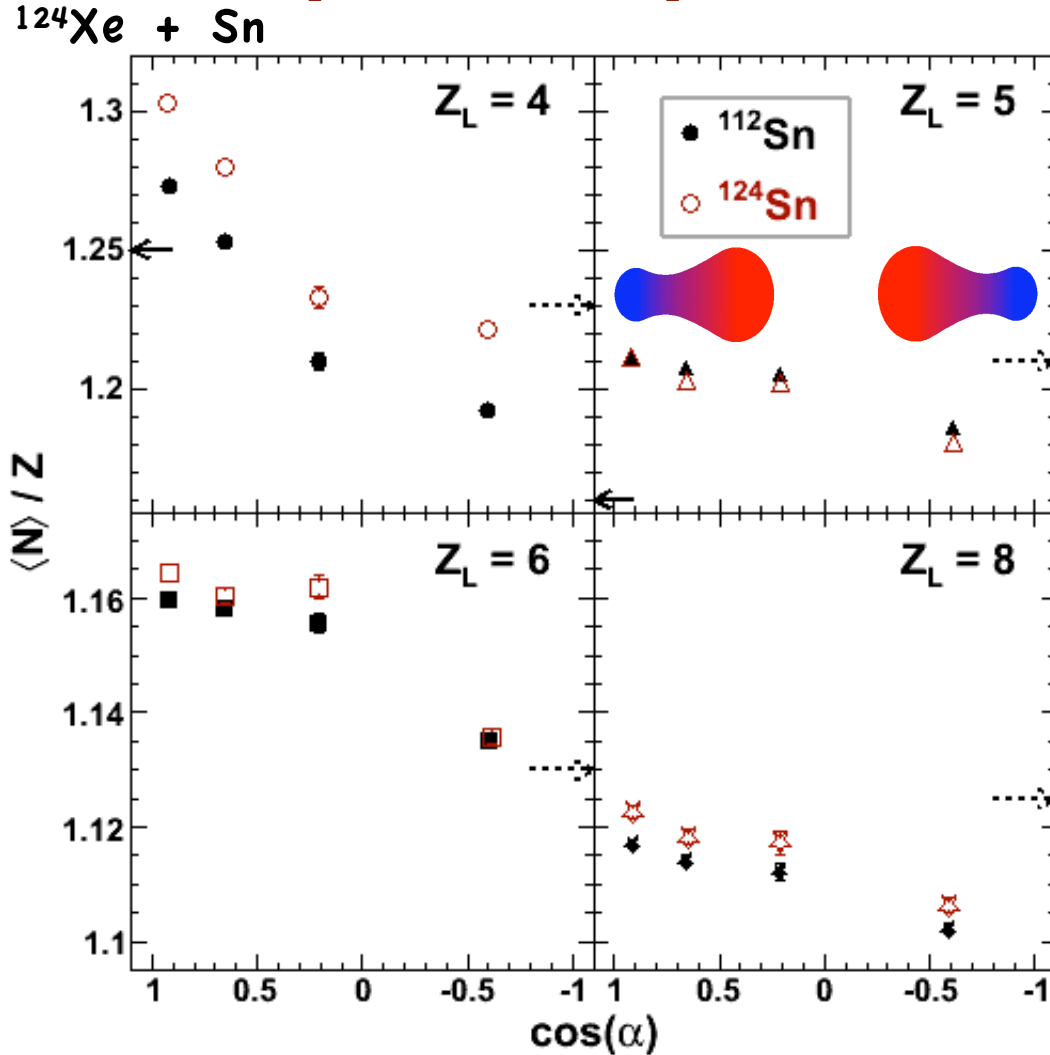
- Backward emission neutron-rich relative to forward emission

Isotopic Composition vs Rotation Angle

 $^{124}\text{Xe} + \text{Sn}$


- Backward emission neutron-rich relative to forward emission
- Fragment neutron content enhanced for larger alignment

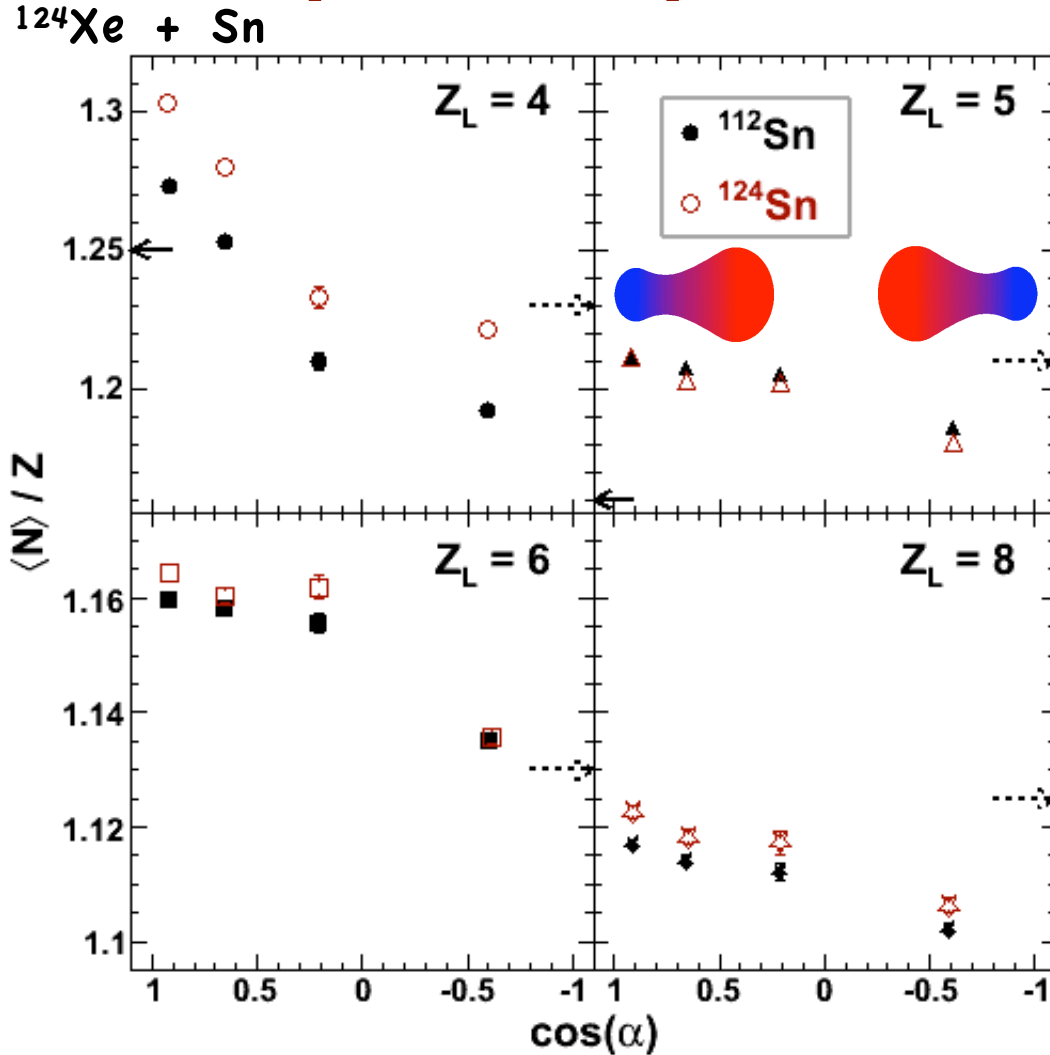
Isotopic Composition vs Rotation Angle



- Backward emission neutron-rich relative to forward emission
- Fragment neutron content enhanced for larger alignment
- Small target effect on the relative neutron composition

	^{124}Xe	^{124}Sn	^{112}Sn
N/Z	1.30	1.48	1.24

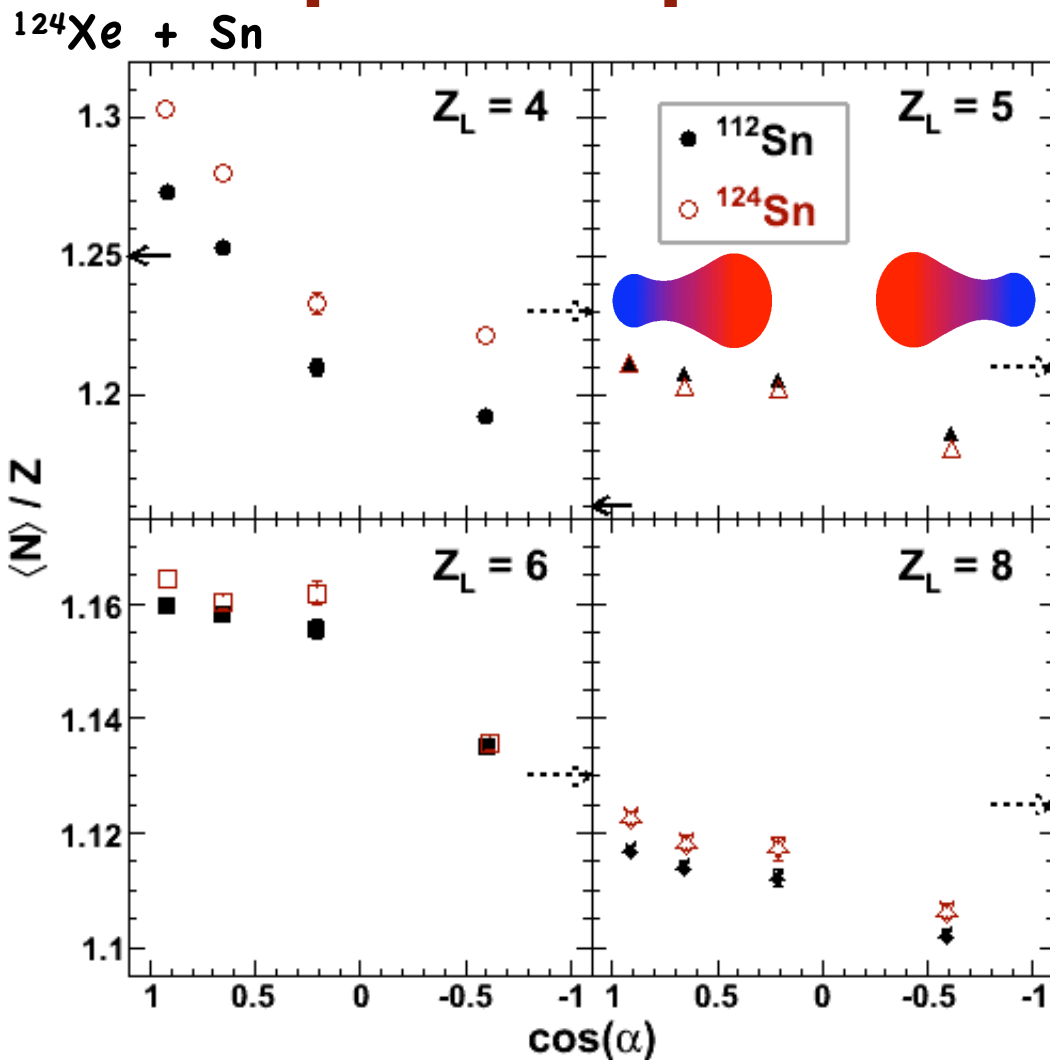
Isotopic Composition vs Rotation Angle



- Backward emission neutron-rich relative to forward emission
- Fragment neutron content enhanced for larger alignment
- Small target effect on the relative neutron composition
- Similar $\langle N \rangle / Z$ observed in ^{124}Sn fragmentation @ 600 MeV/A*

	^{124}Xe	^{124}Sn	^{112}Sn
N/Z	1.30	1.48	1.24

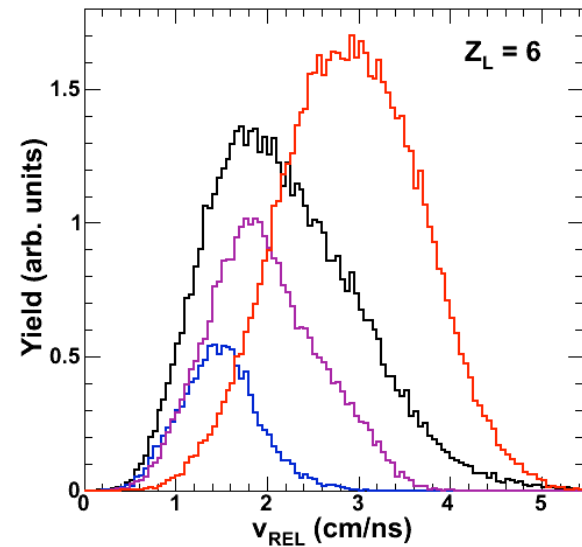
Isotopic Composition vs Rotation Angle



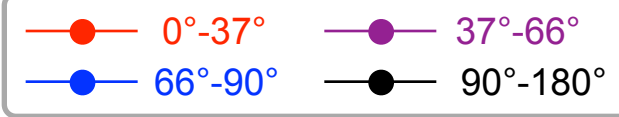
- Backward emission neutron-rich relative to forward emission
- Fragment neutron content enhanced for larger alignment
- Small target effect on the relative neutron composition
- Similar $\langle N \rangle / Z$ observed in ^{124}Sn fragmentation @ 600 MeV/A*
- Same trend observed for $Z=5-8$ for $^{124}\text{Sn} + ^{64}\text{Ni}$ @ 35 MeV/A[©]

	^{124}Xe	^{124}Sn	^{112}Sn
N/Z	1.30	1.48	1.24

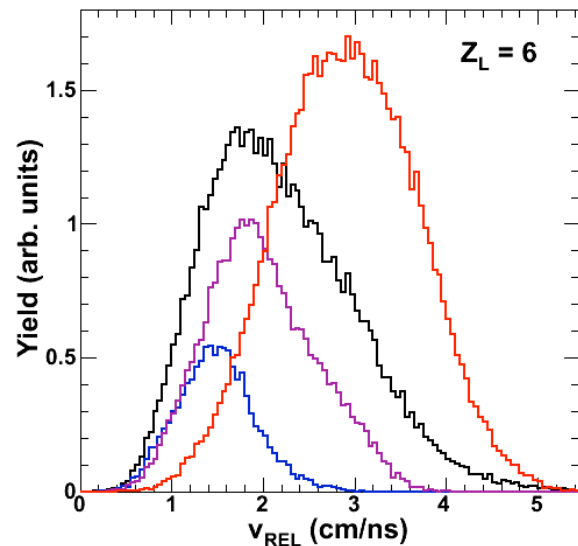
Relative Velocity Dependence



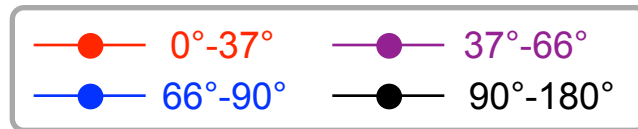
- Larger v_{REL} observed for larger alignment



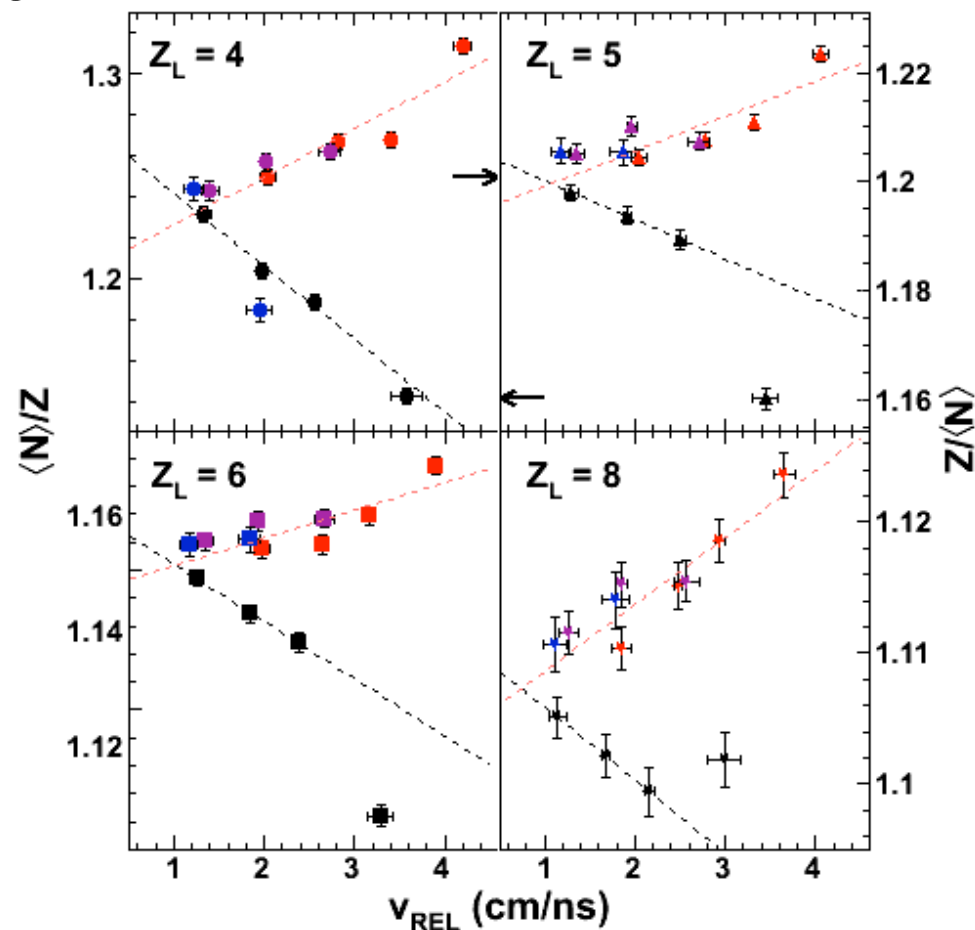
Relative Velocity Dependence



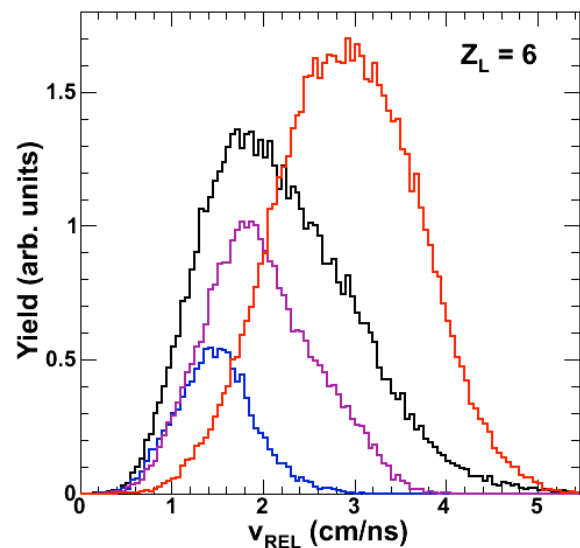
- Larger v_{REL} observed for larger alignment



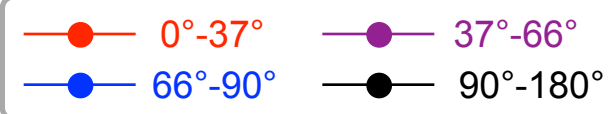
- $\langle N \rangle / Z$ decreases with v_{REL} for forward decay (Coulomb effect)
- $\langle N \rangle / Z$ increases with v_{REL} for backward decay



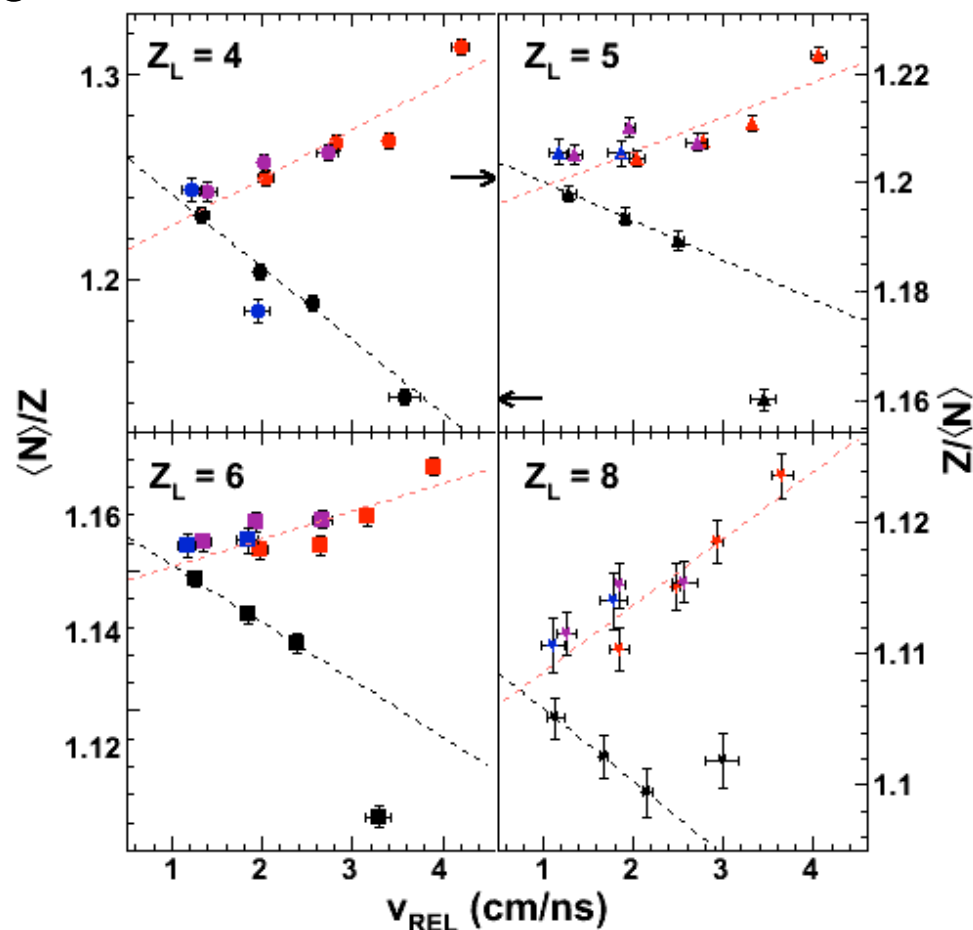
Relative Velocity Dependence



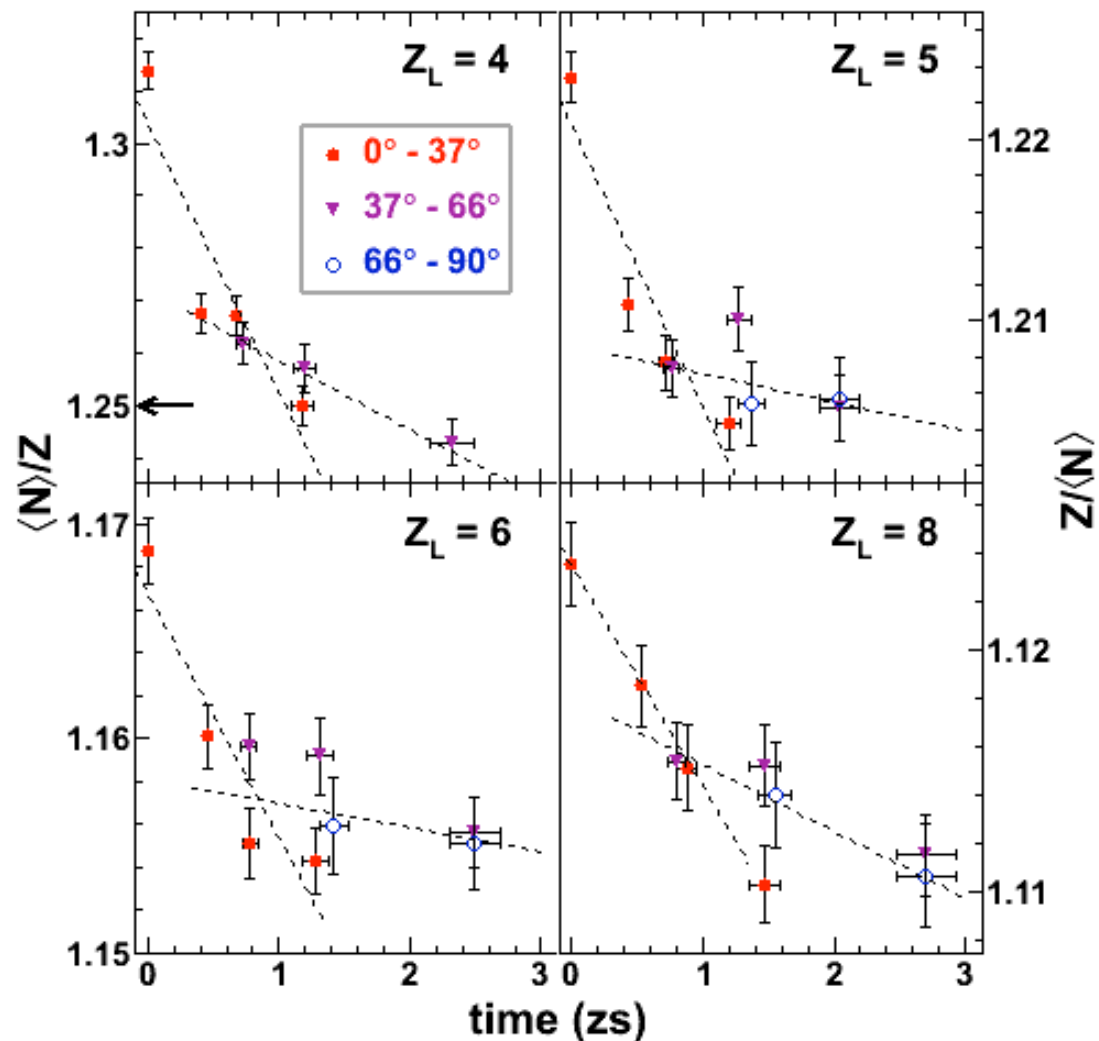
- Larger v_{REL} observed for larger alignment



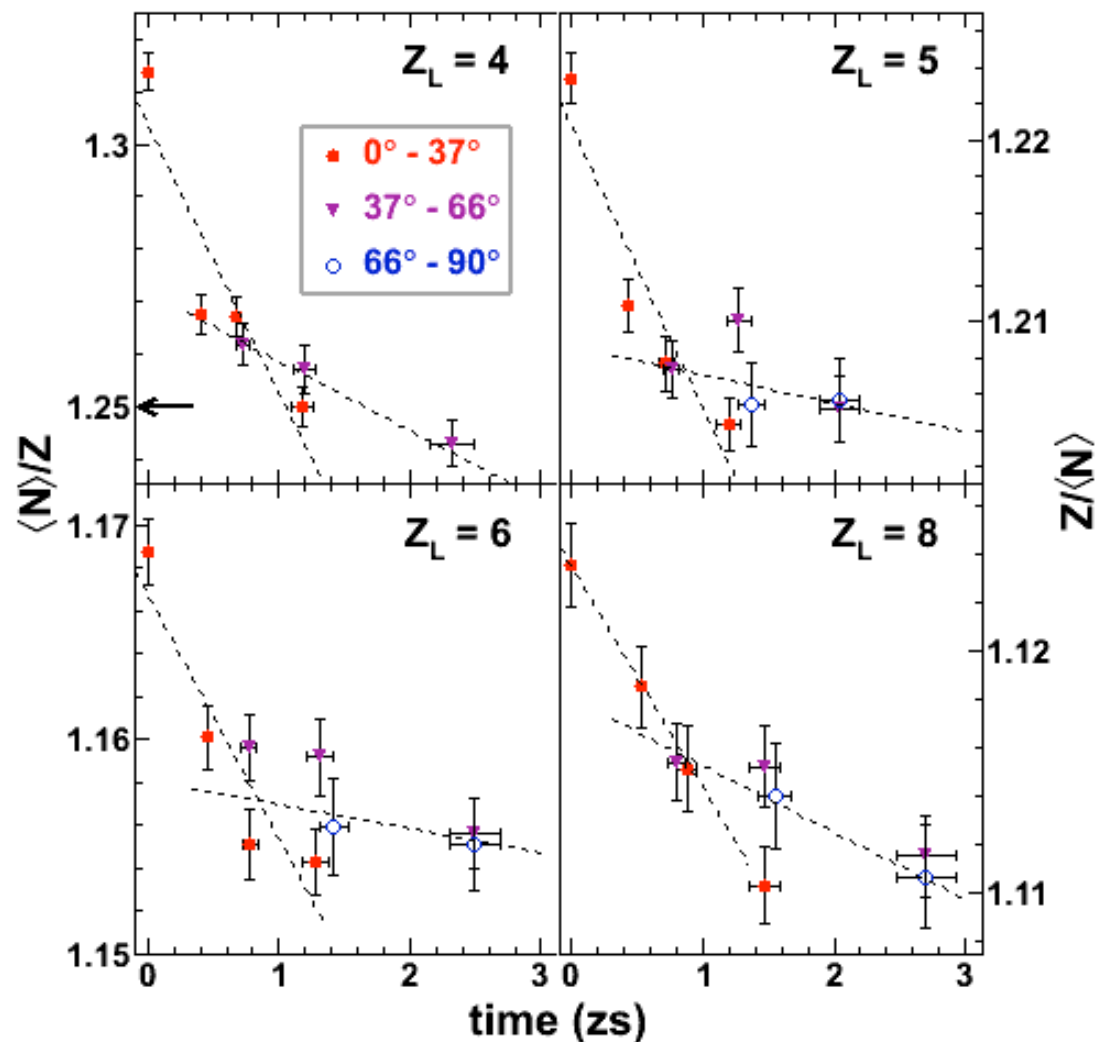
- $\langle N \rangle / Z$ decreases with v_{REL} for forward decay (Coulomb effect)
- $\langle N \rangle / Z$ increases with v_{REL} for backward decay
- All backward decays show the same dependence with v_{REL}



N/Z Time Dependence

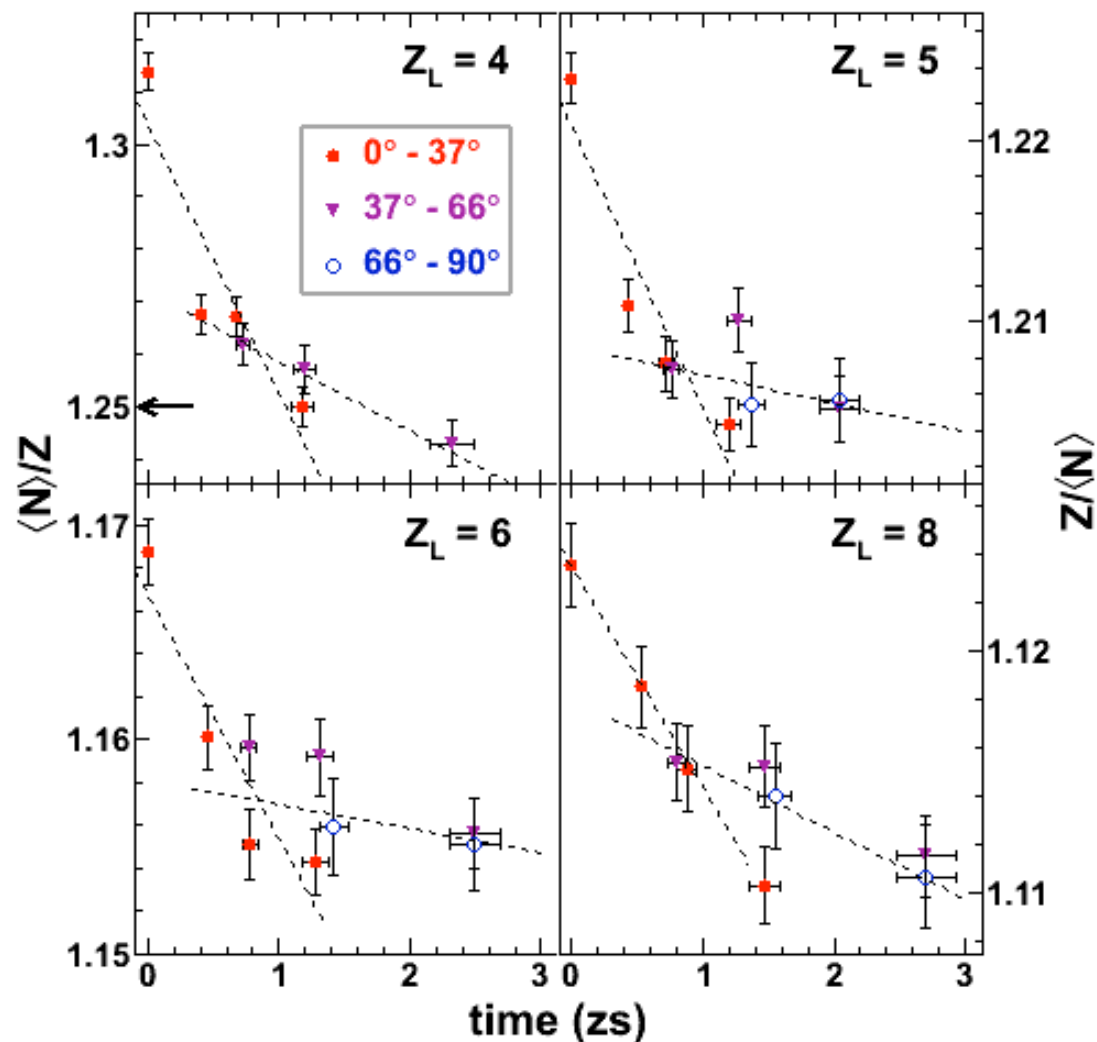
 $^{124}\text{Xe} + ^{112}\text{Sn}$


N/Z Time Dependence

 $^{124}\text{Xe} + ^{112}\text{Sn}$


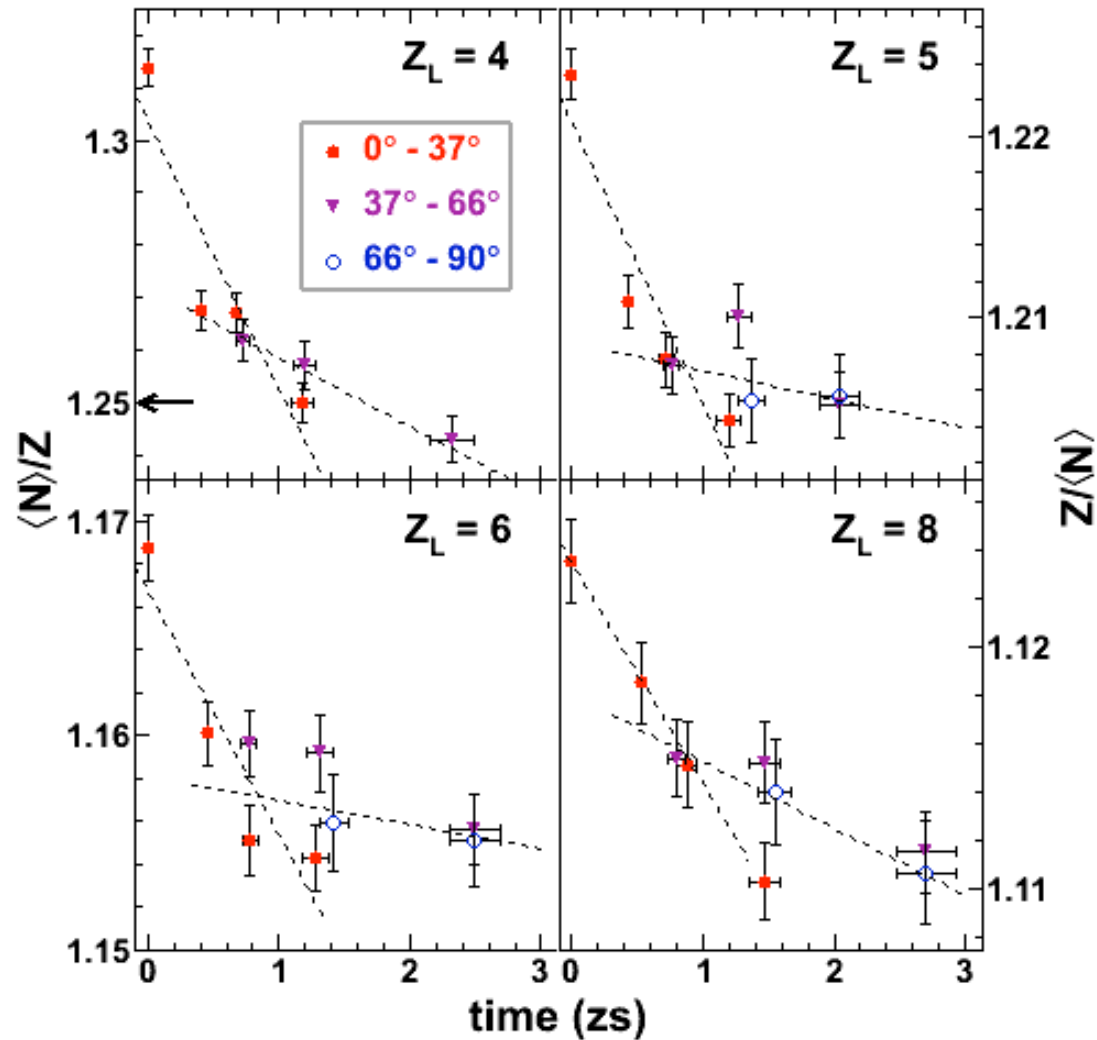
- $Z_L = 4$
- Strong time dependence
- Two components

N/Z Time Dependence

 $^{124}\text{Xe} + ^{112}\text{Sn}$


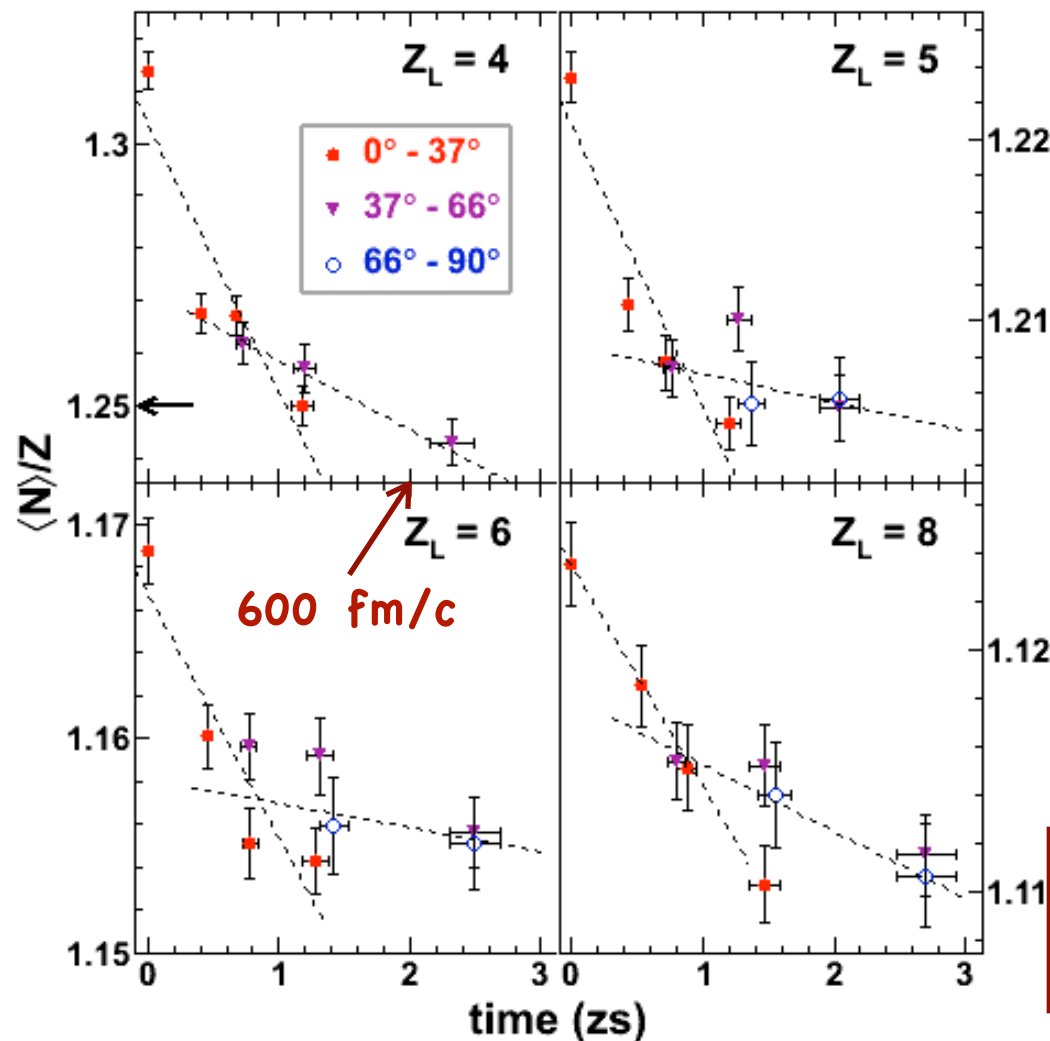
- $Z_L = 4$
 - Strong time dependence
 - Two components
- $Z_L = 5, 6$
 - Time dependence not as pronounced as for $Z_L = 4$

N/Z Time Dependence

 $^{124}\text{Xe} + ^{112}\text{Sn}$


- $Z_L = 4$
 - Strong time dependence
 - Two components
- $Z_L = 5, 6$
 - Time dependence not as pronounced as for $Z_L = 4$
- $Z_L = 8$
 - Similar dependence for both short and long times

N/Z Time Dependence

 $^{124}\text{Xe} + ^{112}\text{Sn}$


- $Z_L = 4$
 - Strong time dependence
 - Two components
- $Z_L = 5, 6$
 - Time dependence not as pronounced as for $Z_L = 4$
- $Z_L = 8$
 - Similar dependence for both short and long times

⇒ Persistence of N/Z equilibration over *long* times

Target Effect

$^{64}\text{Zn} + ^{27}\text{Al}, ^{64}\text{Zn}, ^{209}\text{Bi} @ 45 \text{ MeV/A}$

Angular coverage: $\theta_{\text{Lab}} = 3.5 - 30^\circ$

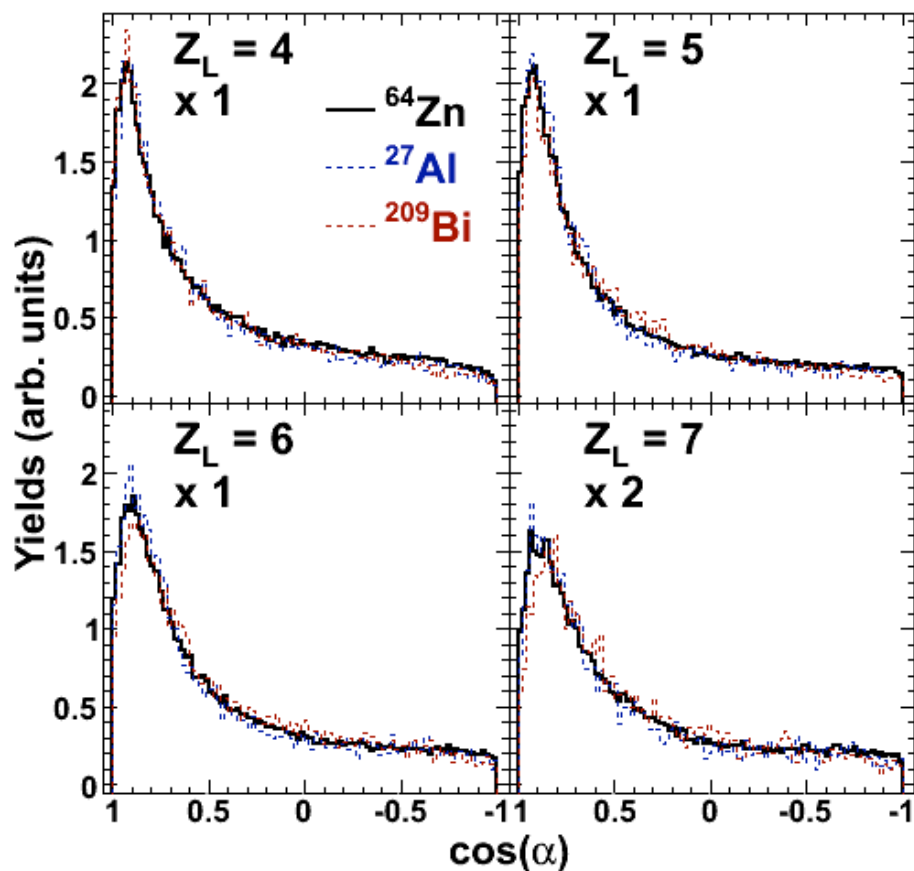
*Work in
Progress*

Target Effect

Work in Progress

$^{64}\text{Zn} + ^{27}\text{Al}, ^{64}\text{Zn}, ^{209}\text{Bi}$ @ 45 MeV/A

Angular coverage: $\theta_{\text{Lab}} = 3.5 - 30^\circ$



→ Aligned decay observed for all targets

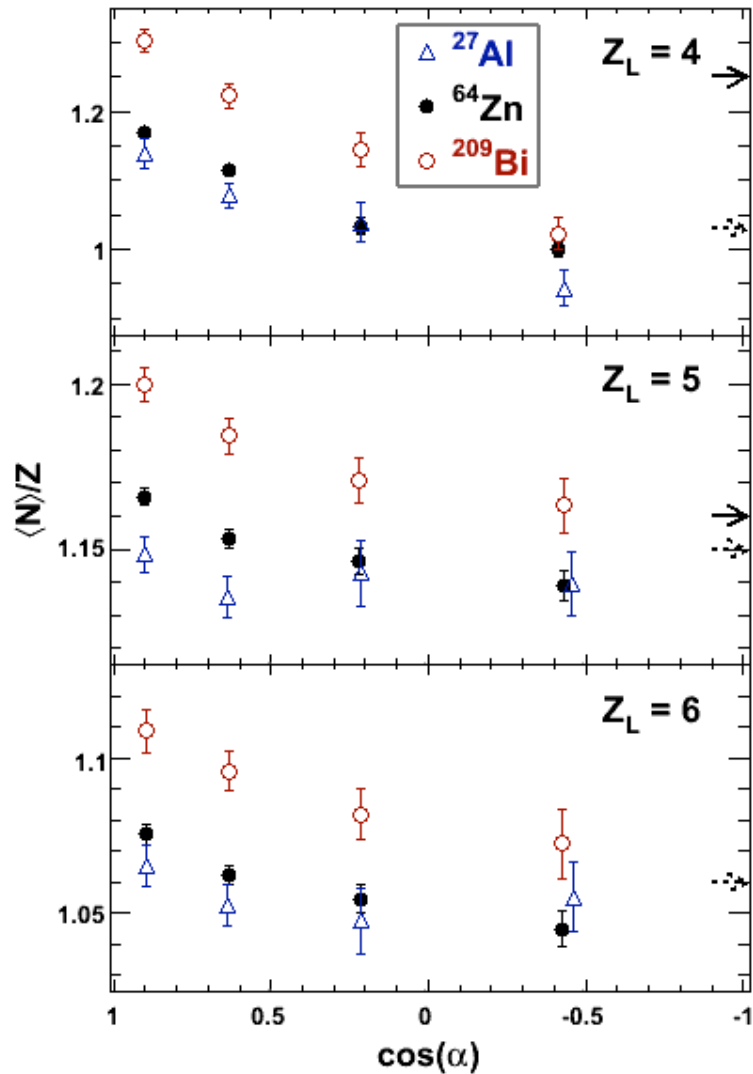
→ Similar angular distributions

 Similar velocity damping and relative velocity

→ Observations suggest that the binary system is prepared in a similar way for all targets

Target Effect on Isotopic Composition

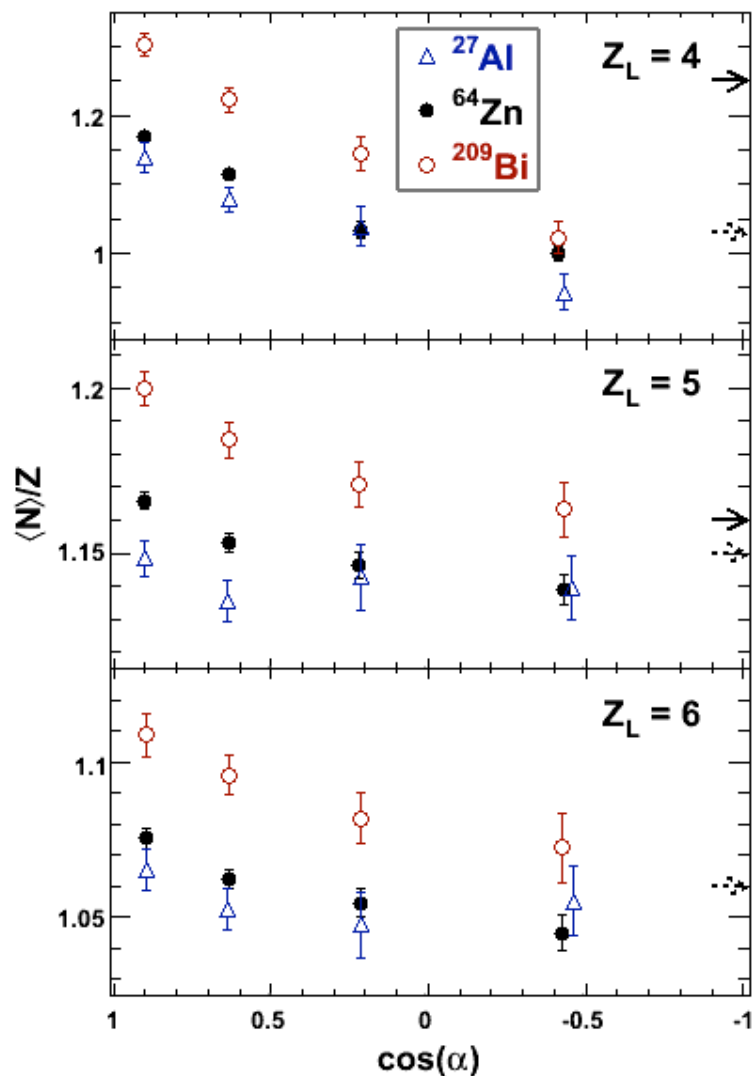
Work in Progress



Target Effect on Isotopic Composition

Work in Progress

- $\langle N \rangle / Z$ dependence on angle



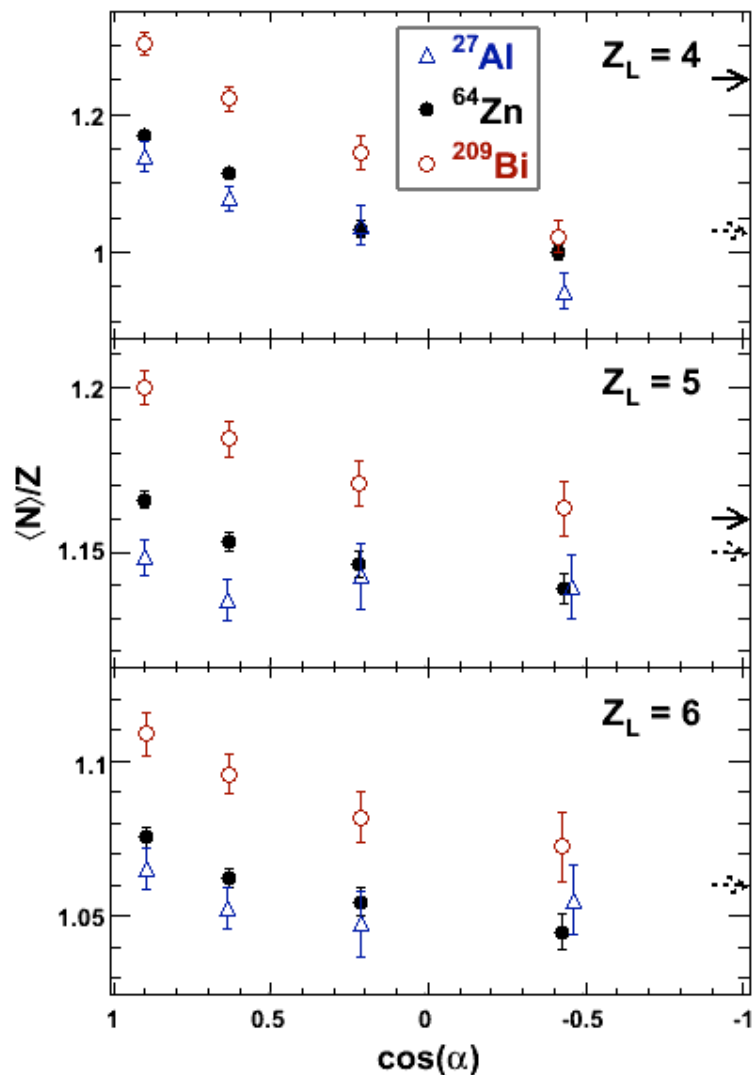
—→ : β -stable

- - - → : C. Sienti *et al.*, PRL 102, 152701 (2009) for ^{124}La ($N/Z = 1.175$)

$N/Z(^{64}\text{Zn})$: 1.13

Target Effect on Isotopic Composition

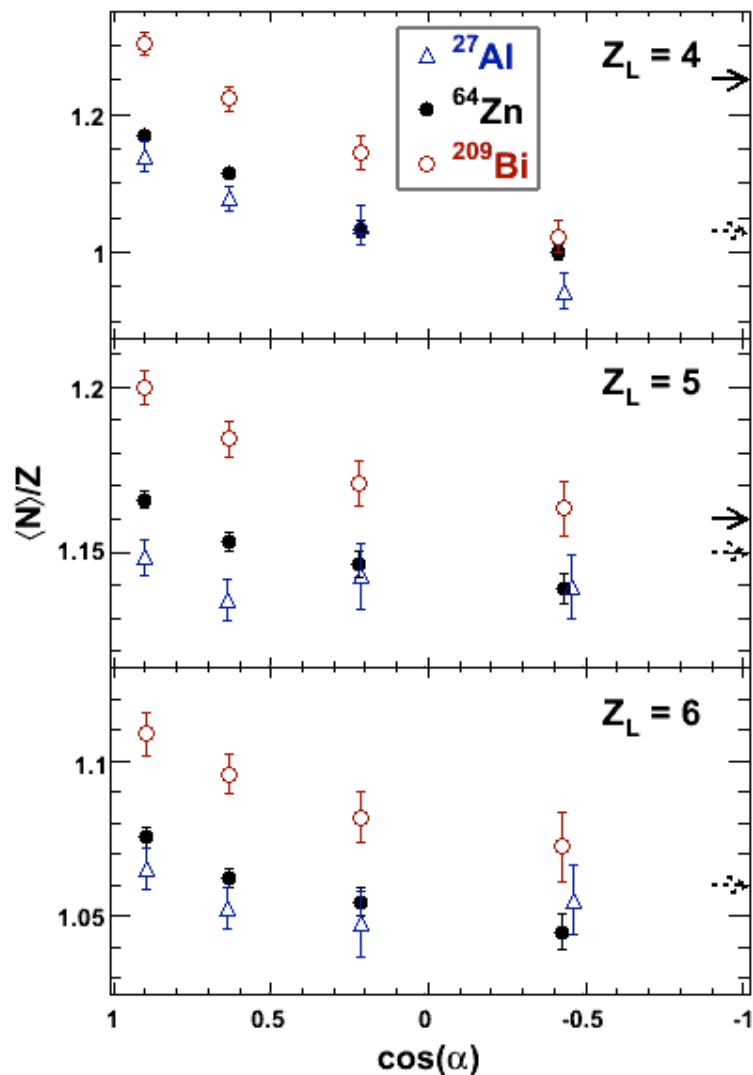
Work in Progress



- $\langle N \rangle / Z$ dependence on angle
- Larger fragment $\langle N \rangle / Z$ for larger target

Target Effect on Isotopic Composition

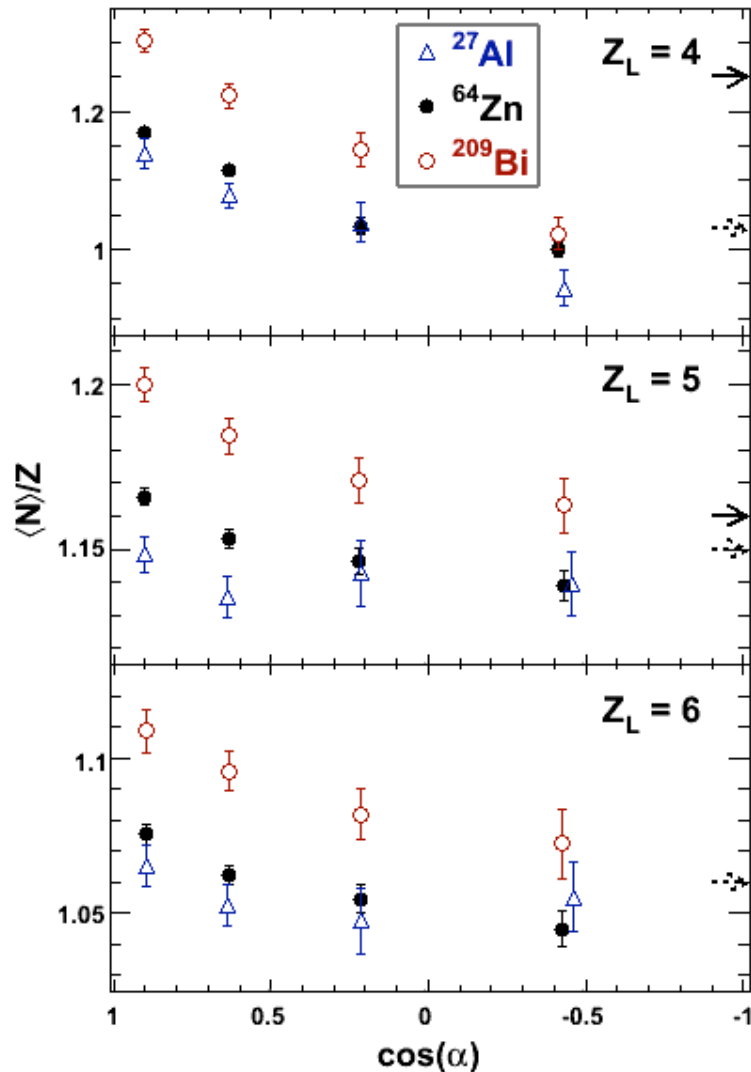
Work in Progress



- $\langle N \rangle / Z$ dependence on angle
- Larger fragment $\langle N \rangle / Z$ for larger target
- $\langle N \rangle / Z$ dependence on v_{REL} stronger for larger Z_{Target} for backward decay

Target Effect on Isotopic Composition

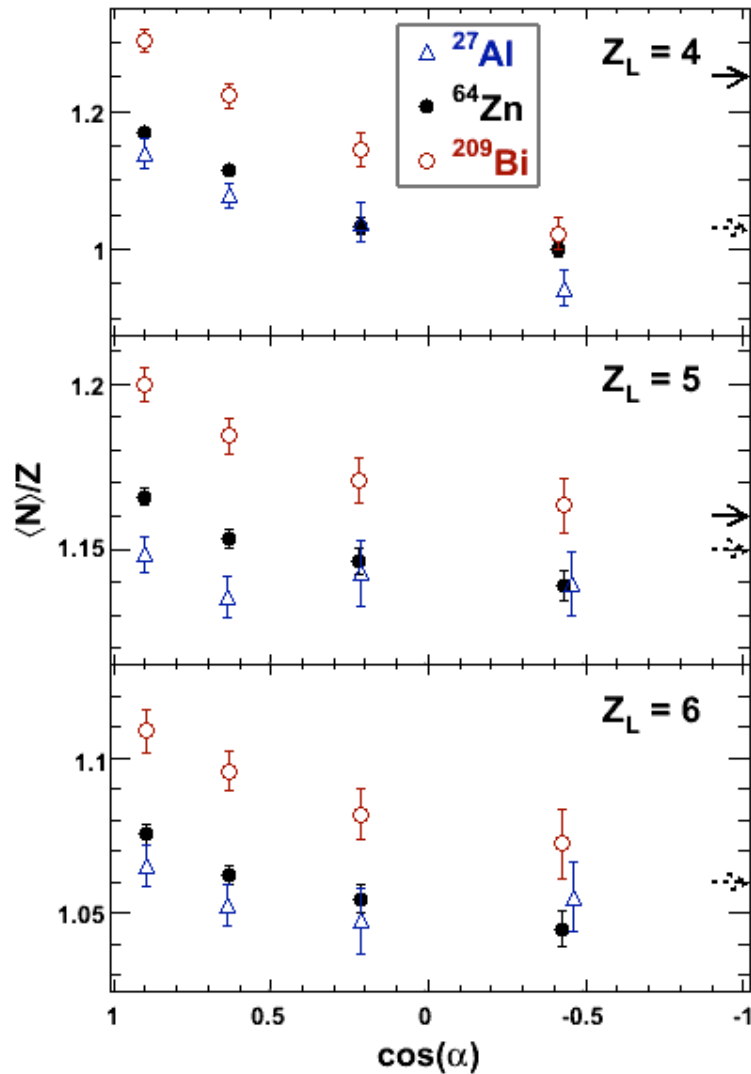
Work in Progress



- $\langle N \rangle / Z$ dependence on angle
- Larger fragment $\langle N \rangle / Z$ for larger target
- $\langle N \rangle / Z$ dependence on v_{REL} stronger for larger Z_{Target} for backward decay
- Possible influences:

Target Effect on Isotopic Composition

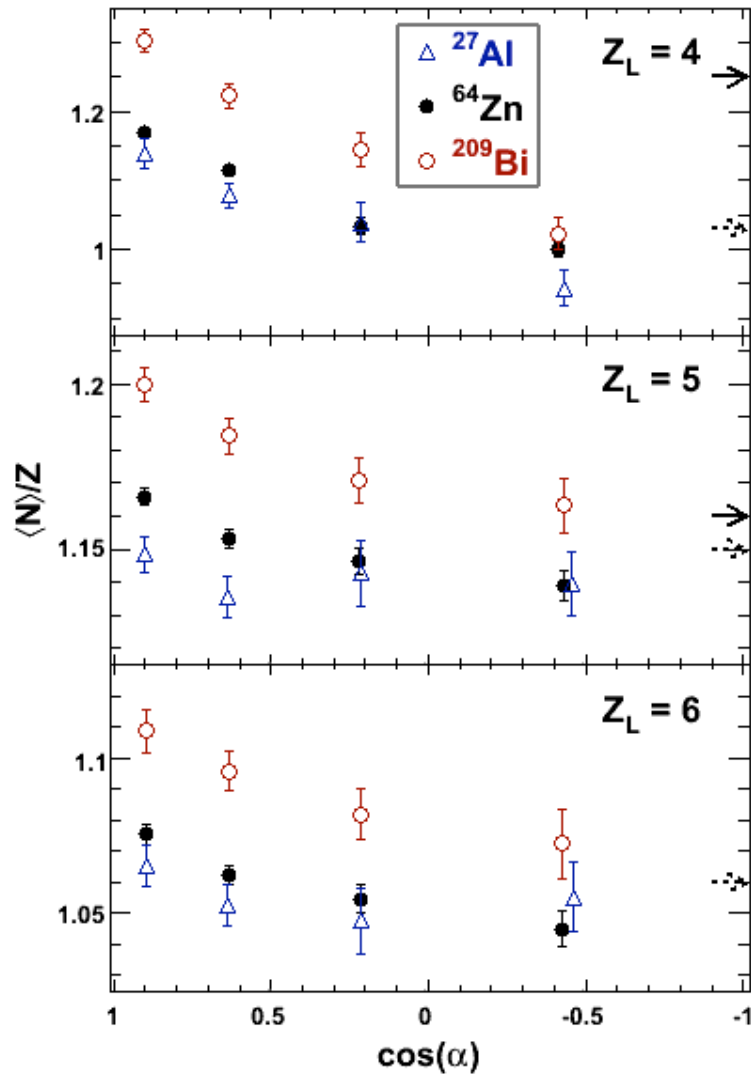
Work in Progress



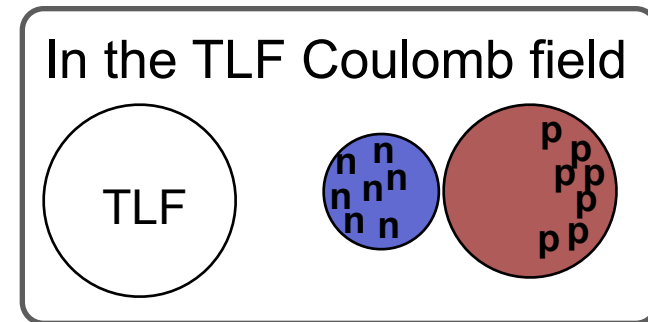
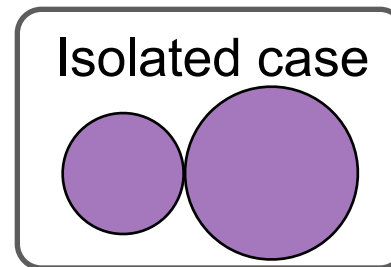
- $\langle N \rangle / Z$ dependence on angle
- Larger fragment $\langle N \rangle / Z$ for larger target
- $\langle N \rangle / Z$ dependence on v_{REL} stronger for larger Z_{Target} for backward decay
- Possible influences:
 1. Target as a source of neutrons

Target Effect on Isotopic Composition

Work in Progress



- $\langle N \rangle / Z$ dependence on angle
- Larger fragment $\langle N \rangle / Z$ for larger target
- $\langle N \rangle / Z$ dependence on v_{REL} stronger for larger Z_{Target} for backward decay
- Possible influences:
 1. Target as a source of neutrons
 2. Polarization induced by the target Coulomb field



Conclusions

Conclusions

- The $\langle N \rangle / Z$ of fragments emitted in dynamical decay is correlated with rotation angle.
- Different v_{REL} dependence are observed for forward and backward emission.
- Similar $\langle N \rangle / Z$ increase with v_{REL} for all backward angles.
- Evolution of $\langle N \rangle / Z$ over 2-3 zs (600-900 fm/c)
- Target effect on $\langle N \rangle / Z$:
 - Small effect if Z is constant and $(N/Z)_{Target}$ changed
 - Large fragment neutron enrichment for larger target (Z & A)

Conclusions

- The $\langle N \rangle / Z$ of fragments emitted in dynamical decay is correlated with rotation angle.
- Different v_{REL} dependence are observed for forward and backward emission.
- Similar $\langle N \rangle / Z$ increase with v_{REL} for all backward angles.
- Evolution of $\langle N \rangle / Z$ over 2-3 zs (600-900 fm/c)
- Target effect on $\langle N \rangle / Z$:
 - Small effect if Z is constant and $(N/Z)_{Target}$ changed
 - Large fragment neutron enrichment for larger target (Z & A)
- Difference in $\langle N \rangle / Z$ time dependence for different Z_L may be related to differences in the initial di-nuclear configuration (different position relative to saddle and scission points).

Conclusions

- The $\langle N \rangle / Z$ of fragments emitted in dynamical decay is correlated with rotation angle.
- Different v_{REL} dependence are observed for forward and backward emission.
- Similar $\langle N \rangle / Z$ increase with v_{REL} for all backward angles.
- Evolution of $\langle N \rangle / Z$ over 2-3 zs (600-900 fm/c)
- Target effect on $\langle N \rangle / Z$:
 - Small effect if Z is constant and $(N/Z)_{Target}$ changed
 - Large fragment neutron enrichment for larger target (Z & A)
- Difference in $\langle N \rangle / Z$ time dependence for different Z_L may be related to differences in the initial di-nuclear configuration (different position relative to saddle and scission points).
- Target effect due to the target as a neutron reservoir? polarization?

Conclusions

- The $\langle N \rangle / Z$ of fragments emitted in dynamical decay is correlated with rotation angle.
- Different v_{REL} dependence are observed for forward and backward emission.
- Similar $\langle N \rangle / Z$ increase with v_{REL} for all backward angles.
- Evolution of $\langle N \rangle / Z$ over 2-3 zs (600-900 fm/c)
- Target effect on $\langle N \rangle / Z$:
 - Small effect if Z is constant and $(N/Z)_{Target}$ changed
 - Large fragment neutron enrichment for larger target (Z & A)
- Difference in $\langle N \rangle / Z$ time dependence for different Z_L may be related to differences in the initial di-nuclear configuration (different position relative to saddle and scission points).
- Target effect due to the target as a neutron reservoir? polarization?
- In the future, use of damped reactions at radioactive beam facilities?

Collaboration and Acknowledgements

- Indiana University: A.B. McIntosh, S. H., K.W. Brown, J. Black, D. Mercier, C.J. Metelko, B. Davin, R. Yanez, R.T. de Souza
- GANIL: A. Chbihi
- GSI: S. Bianchin, C. Schwarz, W. Trautmann
- Université Laval, Québec: M.O. Frégeau, J. Gauthier, F. Grenier, J. Moisan, R. Roy, D. Thériault
- Western Michigan University: M. Famiano
- Texas A&M University: S. Yennello's group

Thanks to:

- The support of the GANIL staff and facility
- The support of the Cyclotron Institute at Texas A&M U.
- The DEMON collaboration

This work was supported by the DOE Office of Science under the Grant No. DEFG02-88ER-40404

